Dalton Transactions

ROYAL SOCIETY OF CHEMISTRY

PAPER

View Article Online
View Journal | View Issue

Cite this: *Dalton Trans.*, 2024, **53**, 2602

Cytotoxic Pt(II) complexes containing alizarin: a selective carrier for DNA metalation†

Rossella Caligiuri,‡[a] Lara Massai,‡[e] Andrea Geri,[e] Loredana Ricciardi,[c] Nicolas Godbert,[a,b] Giorgio Facchetti,*[f] Maria Giovanna Lupo,[g] Ilaria Rossi,[h] Giulia Coffetti,[f] Martina Moraschi,[f] Emilia Sicilia,[d] Vincenzo Vigna,[d] Luigi Messori,[e] Nicola Ferri,[g,i] Gloria Mazzone,*[d] Iolinda Aiello*[a,b,c] and Isabella Rimoldi[f]

Received 20th November 2023,
Accepted 3rd January 2024

DOI: 10.1039/d3dt03889k

rsc.li/dalton

Many efforts have been made in the last few decades to selectively transport antitumor agents to their potential target sites with the aim to improve efficacy and selectivity. Indeed, this aspect could greatly improve the beneficial effects of a specific anticancer agent especially in the case of orphan tumors like the triple negative breast cancer. A possible strategy relies on utilizing a protective leaving group like alizarin as the Pt(II) ligand to reduce the deactivation processes of the pharmacophore enacted by Pt resistant cancer cells. In this study a new series of neutral mixed-ligand Pt(II) complexes bearing alizarin and a variety of diamine ligands were synthesized and spectroscopically characterized by FT-IR, NMR and UV–Vis analyses. Three Pt(II) compounds, *i.e.*, **2b**, **6b** and **7b**, emerging as different both in terms of structural properties and cytotoxic effects (not effective, 10.49 ± 1.21 μM and 24.5 ± 1.5 μM, respectively), were chosen for a deeper investigation of the ability of alizarin to work as a selective carrier. The study comprises the *in vitro* cytotoxicity evaluation against triple negative breast cancer cell lines and ESI-MS interaction studies relative to the reaction of the selected Pt(II) complexes with model proteins and DNA fragments, mimicking potential biological targets. The results allow us to suggest the use of complex **6b** as a prospective anticancer agent worthy of further investigations.

Introduction

One of the greatest successes of medicinal inorganic chemistry is the discovery of Pt(II) anticancer agents, medically used for over 30 years in the treatment of various tumours.[1–4] Three anticancer Pt(II)-based drugs (cisplatin, carboplatin and oxaliplatin) are in clinical use worldwide, while an additional four are exclusively approved in selected countries (nedaplatin and miriplatin in Japan, lobaplatin in China and heptaplatin in South Korea) (Fig. 1).[5]

Although some details of their mechanism of action are still to be clarified, it is well known that the main anticancer activity of most of the Pt(II) drugs arises from their direct interaction with DNA. Generally, these compounds – beyond nucleic acids – display numerous additional intracellular targets as biomolecules containing nitrogen, sulphur, and oxygen atoms (mostly peptides and proteins), such as ribonucleic acids, thiols, glutathione and phospholipids, causing their systemic toxicity.[6–8]

The lack of tumor selectivity, the associated side effects and acquired drug resistance have greatly limited the therapeutic application of these drugs. To improve the efficacy of Pt(II)-based compounds, the design and synthesis of new classes of

[a]*MAT-INLAB, LASCAMM CR-INSTM, Unità INSTM della Calabria, Dipartimento di Chimica e Tecnologie Chimiche, Università della Calabria, Ponte Pietro Bucci Cubo 14C, Arcavacata di Rende (CS), 87036, Italy. E-mail: iolinda.aiello@unical.it*
[b]*LPM-Laboratorio Preparazione Materiali, STAR-Lab, Università della Calabria, Via Tito Flavio, 87036 Rende (CS), Italy*
[c]*CNR-Nanotec, UoS di Cosenza, Dipartimento di Fisica, Università della Calabria, 87036 Rende (CS), Italy*
[d]*Dipartimento di Chimica e Tecnologie Chimiche, Università della Calabria, Ponte Pietro Bucci Cubo 14C, Arcavacata di Rende (CS), 87036, Italy. E-mail: gloria.mazzone@unical.it*
[e]*Department of Chemistry, University of Florence, Via della Lastruccia 3-13, 50019 Sesto Fiorentino, Italy*
[f]*Department of Pharmaceutical Sciences, University of Milan, Via Venezian 21, 20133 Milano, Italy. E-mail: giorgio.facchetti@unimi.it*
[g]*Department of Medicine, University of Padova, Italy*
[h]*Department of Pharmaceutical and Pharmacological Sciences, University of Padova, Italy*
[i]*Veneto Institute of Molecular Medicine, Padua, Italy*

†Electronic supplementary information (ESI) available. See DOI: https://doi.org/10.1039/d3dt03889k

‡These authors contributed equally to this work.

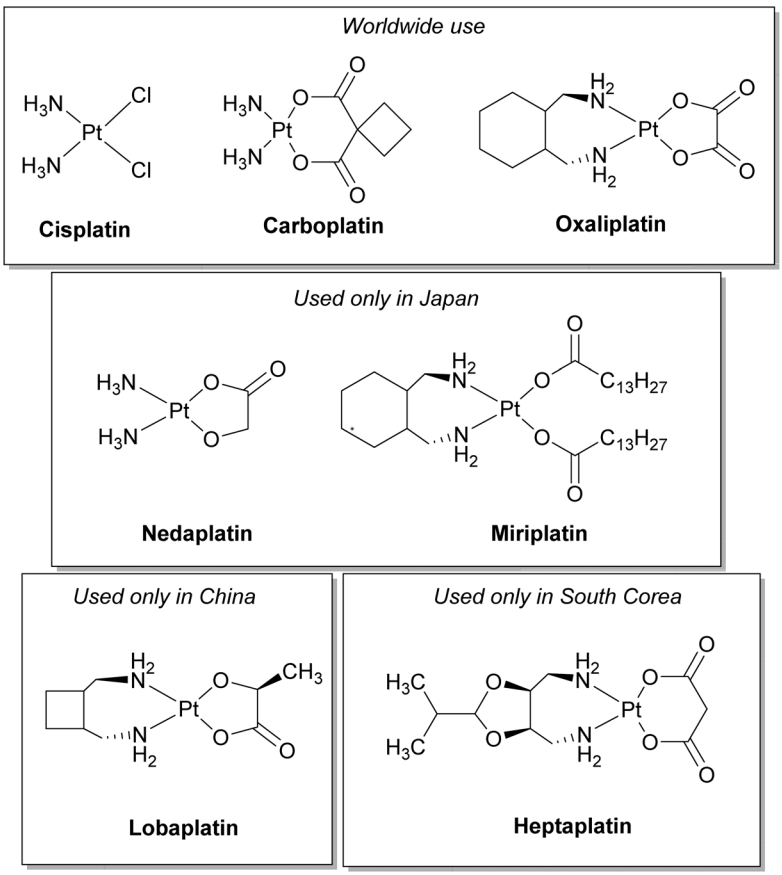

Fig. 1 Chemical structures of approved chemotherapeutic Pt(II) based drugs.

these compounds were focused on the decrease in systemic toxicity through *in situ* activation. With the aim to improve cancer therapy, including receptor targeting, selective drug delivery and design of prodrugs, a wide range of functional Pt (IV) and Pt(II)-based drugs have been studied by applying different synthetic strategies.[9–18]

Based on our long experience in the development of synthetic routes to afford both neutral and ionic complexes of the platinum group,[19–22] we recently synthesized and studied novel charged platinum complexes exhibiting comparable cytotoxicity to cisplatin in particular against the triple negative breast cancer cell line (MDA-MB-231).[23–25] Thus, we focused our attention on MDA-MB-231 known for being a highly aggressive, invasive and poorly differentiated triple-negative breast cancer (TNBC) cell line as it lacks estrogen receptor (ER) and progesterone receptor (PR) expression, as well as HER2 (human epidermal growth factor receptor 2) amplification. For these reasons, antitumoral drugs towards this specific cell line are highly needed and searched for.[26,27]

In the first study, we reported on the synthesis and cytotoxic activity of a series of Pt(II) complexes using 8-aminoquinoline and its chiral 5,6,7,8-tetrahydro-derivatives as chelating ligands.[2] Afterwards, we studied two different series of anionic cyclometalated Pt(II) complexes bearing two different (O^O) chelated ligands, tetrabromocatechol $(BrCat)^{2-}$ and alizarin (aliz).[23] In both studies, promising novel anticancer candidates were identified, showing that both the cycloplatinated amine ligands and the aliz ancillary ligand could induce favorable antitumoral activities in the resulting Pt(II) complexes. On this basis, we decided to combine the main structural features, matching the chelating amine ligands with aliz as the leaving group.

The choice of the leaving group has also been proven to deeply influence the cytotoxicity of the platinum-based chemotherapeutics. The necessity to improve the stability of cisplatin together with the idea to introduce selectivity toward specific tumor cell lines has been realized by substituting the chloride atoms in cisplatin with O,O dicarboxylate groups leading indeed to the more stable carboplatin and oxaliplatin. Based on these important achievements, a series of Pt(II) complexes bearing different pyridylmethylamine N,N ligands both in the form of oxalate and cyclobutanedicarboxylate complexes were prepared. Among them, Oxamusplatin cytotoxicity was demonstrated to be the most potent of the series towards breast adenocarcinoma (MCF-7, IC_{50} = 8.1 ± 0.8 μM) and metastatic prostate carcinoma (DU-145, IC_{50} = 21 ± 1 μM). These complexes also exhibited a better selectivity, even better than that of oxaliplatin, highlighting the importance of finding the perfect match between the nitrogen diamine ligands and the O,O leaving groups.[28]

Recently Pt(II) anticancer agents containing differently substituted O^O ferrocenylbutane-1,3-diones as leaving ligands were synthesized with the aim to modulate the reactivity towards deactivating biomolecules. This study is of relevance in showing the effect of the leaving group on substantially changing the pharmacokinetic and pharmacodynamic processes of the diamino-Pt fragment. Due to the need for increasing pharmacokinetic stability and the selectivity toward cisplatin-resistant cancer cells, Pt(IV) complexes could be synthesized as well and take advantage of the presence of oxygenated ligands in axial positions usually endowed with biological properties.[29,30] Converesly to what described above, another recent example in the literature provides the use of α-hydroxyl carboxylate as the leaving group as in nedaplatin and lobaplatin in view of increasing both the anticancer potency and expanding the nonselective cytotoxicity of platinum chemotherapeutics. This series of 3-hydroxyacrylatoplatinum(II) complexes containing Michael acceptors as leaving groups afforded anticancer complexes with similar activity to oxaliplatin but with a better safety profile *in vivo*.[31]

However, the use of O,O leaving groups different from the popular dicarboxylates for the synthesis of platinum complexes endowed with a new biological profile remains largely unexplored. In this regard, the catechol moiety in alizarin as a dichelating O,O leaving ligand in platinum complexes should represent a truly novel approach for the development of anticancer drugs with higher selectivity.

Indeed, herein we report a series of neutral Pt(II) complexes with the general formula [(N^N)Pt(aliz)], **1b–9b**. Specifically, the coordination sphere comprises an (N^N) neutral bidentate ligand and aliz as the O^O ligand. This set of (N^N) spectator ligands was selected with the aim of probing the influence of the structural and, therefore, electronic features of the ligands on the cytotoxic activity. Furthermore, the (N^N) ligands were also chosen because of their differences in hydrophobicity, steric bulk, and ligand orientation (Fig. 2).[32–34]

In particular, the starting ligand to be considered for this study is 1,2-diaminoethane (**L1**). We decided to extend the series by adding 1,2-phenylenediamine (**L2**), which maintained invariant the two NH_2 chelating groups but introduced a greater rigidity into the resulting metallocycle. To form a second subclass of the series, we chose 2-picolylamine (**L3**) that with respect to 1,2-diaminoethane introduces the sp^2 hybridized nitrogen atom of the pyridine ring in place of the second NH_2 functional group. This subclass was completed with three aminoquinoline derivatives differing in their substituents or in aromaticity, namely: 5,6,7,8-tetrahydro-8-aminoquinoline (**L4**), 2-methyl-5,6,7,8-tetrahydro-8-aminoquinoline (**L5**) and 8-aminoquinoline (**L6**). Finally, the series was completed by introducing two pyridinyl nitrogen atoms through

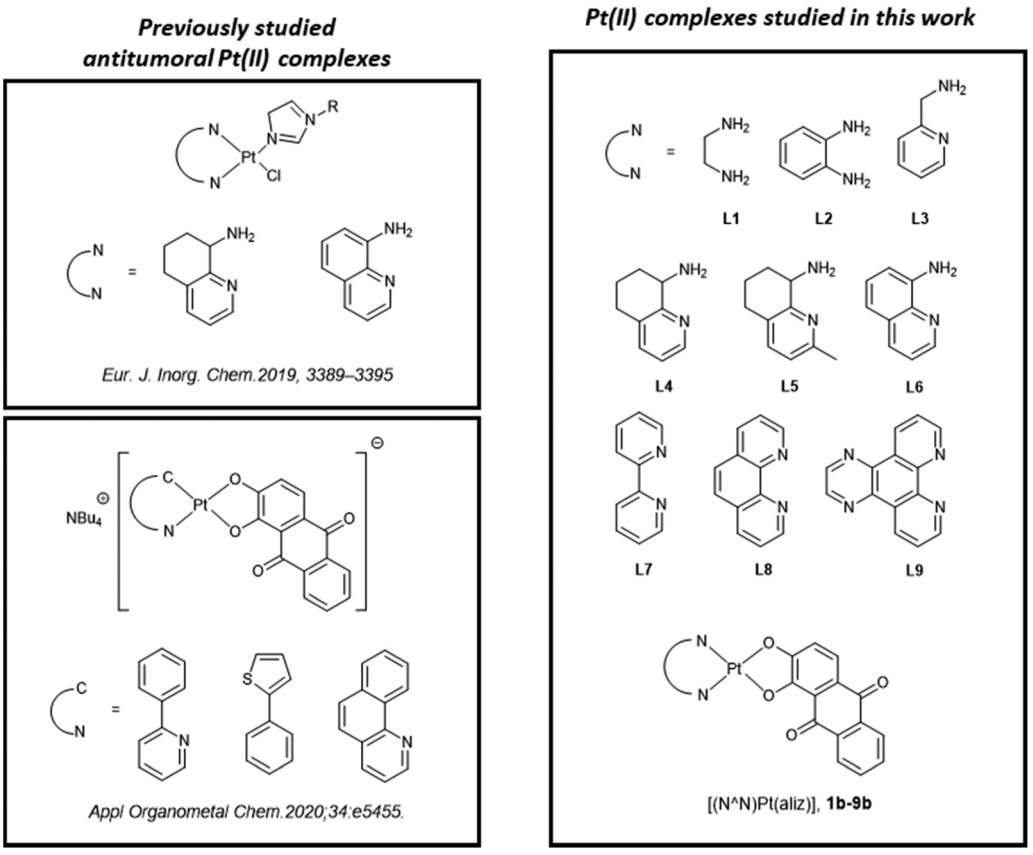

Fig. 2 Chemical structures: on the left panel, literature homologous Pt(II) complexes previously studied; on the right panel, selected ligands (**L1–L9**) and related Pt(II) complexes (**1b–9b**) containing alizarin, objects of the present study.

adding to the ligand pool the ligands 2,2′-bipyridine (**L7**), 1,10-phenanthroline (**L8**), and pyrazino[2,3-*f*][1,10]phenanthroline (**L9**), which were selected not only because of their differences in rigidity and extension of aromaticity, but also because their biological activity is well known (Fig. 2).[35–37]

Several studies have been conducted to investigate the effect of the non-leaving (N^N) ligands on the reactivity of Pt (II) antitumor drugs and, also, on the rate of ligand exchange for the formation of Pt(II) diaqua complexes, which are important because they represent the reactive species in the crucial step of cisplatin binding to DNA.[33,38,39]

In order to explore how their properties are influenced by the use of (N^N) ligands, the $[(NH_3)_2Pt(aliz)]$ complex was also synthesized.[25]

Experimental section

Materials

All commercially available chemicals were purchased from Sigma-Aldrich or Alfa Aesar and used without further purification. $[(N^N)PtCl_2]$ precursors **1a**, **3a**, **8a**, **9a**[40–43] and **4a–6a**[24,44] were synthesized following already reported methods. DMEM, trypsin-EDTA, penicillin, streptomycin, non-essential amino acid solution, fetal calf serum (FCS), disposable culture flasks and Petri dishes were purchased from Euroclone S.p.A. (Pero, Milan, Italy).

Physical methods

Melting points were determined with a Leica DMLP polarizing microscope equipped with a Leica DFC280 camera and a CalCTec (Italy) heating stage.[45] Elemental analyses were performed with a PerkinElmer 2400 analyzer CHNS/O. FT-IR spectra (KBr pellets) were recorded on a Spectrum One PerkinElmer FT-IR spectrometer. ^{1}H and ^{13}C NMR spectra were recorded on a Bruker Avance 300 MHz spectrometer and in DMSO-d_6 with TMS as the internal standard.[46] ESI-MS analyses were performed by using a Thermo Finnigan (MA, USA) LCQ Advantage system MS spectrometer with an electrospray ionisation source and an 'Ion Trap' mass analyser. The MS spectra were obtained by direct infusion of a sample solution in MeOH under ionisation, ESI positive. For UV–Visible spectroscopy, spectrofluorimetric-grade solvents were used for the preparation of all solutions. The buffer solution (pH 7.4) was prepared by dissolving one phosphate buffered saline tablet (Sigma-Aldrich) in 200 mL of water. Compounds **1b–9b** were dissolved in DMSO and then diluted to reach a final concentration of 1×10^{-5} M in DMSO/buffer solution (DMSO 0.5% v/v). A PerkinElmer Lambda 900 spectrophotometer was employed to record the UV–Visible absorption spectra, using 10 mm path-length quartz cuvettes.

Preparation of $[(N^N)PtCl_2]$ complexes 2a, 6a, and 7a

Potassium tetrachloroplatinate (3.47 mmol) was dissolved in 10 mL of distilled water in a Schlenk tube under a nitrogen atmosphere and to this 3.47 mmol of the diamine ligand **L1–L9** was added. The mixture was acidified with 6 M HCl (4.62 mL) and heated under reflux overnight. After cooling to room temperature, the product was collected as a differently colored solid, washed extensively with water followed by small amounts of diethyl ether and dried under vacuum. The complexes were completely characterized, and the data obtained were in accordance with those reported in the literature.

$[(L2)PtCl_2]$, 2a. Yield 80%; m.p. >250 °C; $C_6H_8Cl_2N_2Pt$ (MW = 372.97): Anal. calcd: C, 19.26; H, 2.16; N, 7.49; found C, 19.63; H, 2.20; N, 7.30. ^{1}H NMR (300 MHz, DMSO-d_6) δ 7.61 (bs, 4H), 7.43–7.40 (m, 2H), 7.30–7.27 (m, 2H) ppm. ^{13}C NMR (101 MHz, DMSO-d_6) δ 143.64, 127.87, 126.47 ppm; MS(ESI): m/z $[M]^+$ calcd 389.16; found 412.08 $[M + Na]^+$; 352.32 $[M - Cl]^+$.

$[(L6)PtCl_2]$, 6a. Yield 98%; m.p. >250 °C; $C_9H_8Cl_2N_2Pt$ (MW = 408.97): Anal. calcd: C, 26.36; H, 1.97; N, 6.83; found C, 26.87; H, 2.06; N, 6.94. ^{1}H NMR (300 MHz, DMF-d_7) δ = 9.67 (dd, J = 5.3, 1.3 Hz, 1H), 8.94 (dd, J = 8.4, 1.3 Hz, 1H), 8.09 (dd, J = 21.3, 7.5 Hz, 2H), 7.96–7.64 (m, 2H), 4.02 (brs, 2H) ppm. ^{13}C NMR (101 MHz, DMF-d_7) δ 149.12, 148.90, 141.99, 138.72, 130.72, 129.11, 128.23, 127.53, 123.74 ppm; MS(ESI): m/z $[M]^+$ calcd 408.97; found 409.23 $[M + H]^+$.

$[(L7)PtCl_2]$, 7a. Yield 92%; m.p. >250 °C; $C_{10}H_8Cl_2N_2Pt$ (MW = 420.97): Anal. calcd: C, 28.45; H, 1.71; N, 6.64; found C, 28.35; H, 1.85; N, 6.49. ^{1}H NMR (300 MHz, DMSO-d_6) δ 9.43 (d, J = 32.6, 19.5 Hz, 1H), 8.58 (d, J = 8.1 Hz, 1H), 8.41 (t, J = 7.8 Hz, 1H), 7.83 (t, J = 6.7 Hz, 1H) ppm. ^{13}C NMR (101 MHz, DMSO-d_6) δ 124.8, 128.3, 141.1, 149.3, 157.9 ppm; MS(ESI): m/z $[M]^+$ calcd 422.17; found 423.08 $[M + H]^+$.

Preparation of $[(N^N)Pt(aliz)]$ complexes 1b–9b

$[(L1)Pt(aliz)]$, 1b. H_2(aliz) (58 mg, 0.24 mmol) was solubilized in 15 mL of degassed ethanol, and KOH (54 mg, 0.96 mmol) was added. After **1a** (80 mg, 0.24 mmol) was suspended, the mixture was stirred for 12 h at r.t. The desired product was filtered off and washed with ethanol, distilled water, dichloromethane, and ethyl ether. Purple solid, yield 67%; m.p. >250 °C; $C_{16}H_{14}N_2O_4Pt$ (MW = 493.38): Anal. calcd: C, 38.95; H, 2.86; N, 5.68%; found: C, 38.92; H, 2.89; N, 5.67%; FT-IR (KBr) ν(cm^{-1}) = 3303s (NH), 3206s (NH), 3063s (CH aromatic), 2995w (CH aliphatic), 1630s (CO), 1587s (CO), 1455s (CC), 1349vs (C–O), 1204m, 716s; ^{1}H NMR (300 MHz, DMSO-d_6) δ 8.12 (pseudo-dd, 2H), 7.75 (m, 2H), 7.52 (d, J = 8.25 Hz, 1H), 6.32 (d, J = 8.49 Hz, 1H), 5.60 (sbr, 4H, –NH_2), 2.48 (s, 4H) ppm; ^{13}C NMR (75 MHz, DMSO-d_6,) δ 186.90, 176.01, 168.72, 155.67, 135.30, 133.13, 132.92, 131.10, 125.35, 125.19, 124.27, 117.87, 113.69, 112.39, 46.54 ppm; MS(ESI): m/z $[M]^+$ calcd 493.38; found 493.01 $[M]^+$.

$[(L2)Pt(aliz)]$, 2b. The reaction conditions were analogous to those reported for **1b**, using **2a** (100 mg, 2.73 mmol), H_2(aliz) (128 mg, 5.34 mmol) and KOH (61 mg, 10.91 mmol). Dark purple solid, yield 88%; m.p. >250 °C; $C_{20}H_{14}N_2O_4Pt$ (MW = 541.42): Anal. calcd: C, 44.37; H, 2.61; N, 5.17%; found: C, 44.40; H, 2.63; N, 5.15%; FT-IR (KBr) ν(cm^{-1}) = 3224sh (NH), 3060w (CH aromatic), 2914vw (CH aliphatic), 1625m (CO), 1584m (CO), 1556s (CC), 1497vs, 1465vs, 1392vs (C–O), 1361m,

1206s, 717s; ^{1}H NMR (300 MHz, DMSO-d_6) δ 8.14 (m, 4H), 7.77 (m, 4H), 7.56 (m, 1H), 6.51 (m, 1H) ppm; ^{13}C NMR (101 MHz, DMSO-d_6) δ 188.41, 178.50, 163.85, 155.83, 154.74, 135.55, 134.54, 133.87, 132.99, 126.67, 126.50, 124.00, 122.22, 119.62, 118.83, 116.93, 115.37 ppm; MS(ESI): m/z $[M]^+$ calcd 541.42; found 408.56 $[M - C_8H_4O_2]^+$.

[(L3)Pt(aliz)], 3b. The reaction conditions were analogous to those reported for **1b**. The reaction was conducted using **3a** (100 mg, 2.67 mmol), H_2(aliz) (128 mg, 5.34 mmol) and KOH (61 mg, 10.70 mmol). The mixture was heated at reflux temperature for 24 hours. Dark blue solid, yield 89%; m.p. >250 °C; $C_{20}H_{14}N_2O_4Pt$ (MW = 541.42): Anal. calcd: C, 44.37; H, 2.61; N, 5.17%; found: C, 44.34; H, 2.59; N, 5.17%; FT-IR (KBr) ν(cm^{-1}) = 3219m (NH), 3185sh (NH), 3117w (CH aromatic), 1624m (CO), 1584m (CO), 1555s (CC), 1497vs, 1461vs, 1391vs (C–O), 1362m, 1206s, 716s; ^{1}H NMR (300 MHz; DMSO-d_6) δ 9.06 (m, 1H), 8.10 (m, 4H), 7.74 (m, 3H), 7.49 (m, 1H), 6.37 (m, 2H, –N*H*$_2$), 4.02 (m, 2H) ppm; ^{13}C NMR (101 MHz, DMSO-d_6) δ 173.08, 170.24, 166.77, 157.40, 149.21, 147.63, 143.38, 142.19, 139.19, 135.89, 134.22, 129.27, 125.78, 125.06, 125.06, 124.67, 123.51, 123.01, 122.31, 122.31, 53.31 ppm; MS(ESI): m/z $[M]^+$ calcd; found 423.32 $[M - C_7H_4O_2]^+$.

[(L4)Pt(aliz)], 4b. [(**L4**)$PtCl_2$], complex **4a** (0.73 mmol) and Ag(CF_3SO_3) (1.46 mmol) were suspended in dimethylformamide (10 mL) and stirred at room temperature for 12 h under a nitrogen atmosphere in the dark. The precipitate was filtered off on Celite and to the resulting solution were added H_2(aliz) (0.73 mmol) and 2 M NaOH (2 eq.). After 5 h, the solvent was evaporated under vacuum and the obtained powder was suspended in 20 mL of acetone. At this point, the mixture was filtered yielding the desired product as a purple solid, yield 58%; m.p. >250 °C; $C_{23}H_{14}N_2O_4Pt$ (MW = 577.06); Anal. calcd: C, 47.84; H, 2.44; N, 4.85; found: C, 47.35; H, 2.50; N, 4.34; FT-IR (KBr) ν(cm^{-1}) = 3486w (N–H), 3062w (CH aromatic), 1623m (CO), 1588s(CC), 1387s(C–O), 1254w, 1225s, 828s, 717vs; ^{1}H NMR (300 MHz, DMSO-d_6) 8.20–8.06 (m, 3H), 7.80–7.70 (m, 3H), 7.42 (d, J = 9.5 Hz, 2H), 6.47 (d, J = 8.0 Hz, 1H), 3.91 (s, 1H), 3.06 (m, 2H), 2.69–2.65 (m, 1H), 2.54 (m, 2H), 2.38–2.29 (m, 1H) ppm. ^{13}C NMR (101 MHz, DMSO-d_6) δ 189.29, 181.08, 153.37, 151.29, 149.32, 141.85, 139.07, 135.61, 134.56, 134.07, 133.36, 130.38, 129.80, 129.32, 128.19, 127.45, 127.22, 126.99, 124.23, 124.00, 121.62, 121.33, 116.76 ppm; MS(ESI): m/z $[M]^+$ calcd 577.46; found 578.09 $[M + H]^+$.

[(L5)Pt(aliz)], 5b. The reaction conditions were analogous to those reported for **4b**. The product was obtained as a purple powder, yield 83%; m.p. >250 °C; $C_{23}H_{18}N_2O_4Pt$ (MW = 581.09); Anal. calcd: C, 47.34; H, 3.45; N, 4.80; found: C, 47.23; H, 3.40; N, 4.77; FT-IR (KBr) ν(cm^{-1}) = 3522w (N–H), 3216w (CH aromatic), 1659m (CO), 1589s (CC), 1398s (C–O), 1252w, 1165w, 828s, 714s; ^{1}H NMR (300 MHz, DMSO-d_6) δ 8.17 (m, 2H), 7.91–7.83 (m, 3H), 7.74 (s, 1H), 7.57 (d, J = 8.2 Hz, 1H), 7.36 (m, 1H), 7.08 (d, J = 8.0 Hz, 1H), 2.87 (s, 3H), 2.83–2.70 (m, 4H), 2.60 (m, 2H) ppm. ^{13}C NMR (101 MHz, DMSO-d_6) δ 178.68, 162.78, 150.90, 149.82, 143.31, 135.86, 135.70, 133.50, 132.59, 126.38, 122.76, 122.29, 120.09, 119.39, 117.39, 117.37, 116.17, 116.13, 114.81, 108.69, 107.92, 107.16, 36.25, 31.25 ppm. MS(ESI): m/z $[M]^+$ calcd 581.49; found 582.33 $[M + H]^+$.

[(L6)Pt(aliz)], 6b. The reaction conditions were analogous to those reported for **4b**. The product was obtained as a purple powder, yield 64%; m.p. 185 °C; $C_{24}H_{20}N_2O_4Pt$ (MW = 595.11); Anal. calcd: C, 48.41; H, 3.39; N, 4.70; found: C, 48.12; H, 3.32; N, 4.67; FT-IR (KBr) ν(cm^{-1}) = 3367w (N–H), 3119w (CH aromatic), 3053w (CH aliphatic), 2890s (CH aliphatic), 1661m (CO), 1587s (CC), 1454w (CH aliphatic), 1399s (C–O), 1287w, 1161w, 830s, 773m, 713m; ^{1}H NMR (300 MHz, DMSO-d_6) δ 9.63–9.43 (m, 1H), 8.86 (dd, J = 8.4, 1.2 Hz, 1H), 8.29–8.16 (m, 2H), 8.02 (dd, J = 8.9, 4.4 Hz, 1H), 7.99–7.88 (m, 3H), 7.76 (m, 2H), 7.71–7.63 (m, 1H), 7.30 (d, J = 8.3 Hz, 1H) ppm. ^{13}C NMR (101 MHz, DMSO-d_6) δ 180.57, 162.76, 159.36, 157.95, 141.40, 140.95, 135.14, 135.13, 134.79, 134.77, 134.07, 132.94, 131.48, 127.09, 126.78, 126.73, 123.26, 121.63, 119.99, 114.35, 36.22, 26.63, 22.98, 20.66 ppm. MS(ESI): m/z $[M]^+$ calcd 595.52; found 596.72 $[M + H]^+$.

[(L7)Pt(aliz)], 7b. The reaction conditions were analogous to those reported for **1**. The reaction was conducted using **7a** (80 mg, 0.19 mmol), H_2(aliz) (45 mg, 0.19 mmol) and KOH (37 mg, 0.76 mmol). Very dark purple solid, yield 88%; m.p. >250 °C; $C_{24}H_{14}N_2O_4Pt$ (MW = 589.46): Anal. calcd: C, 48.90; H, 2.39; N, 5.75%; found: C, 48.91; H, 2.42; N, 5.73%; FT-IR (KBr) ν(cm^{-1}) = 3085w (CH aromatic), 3059w (CH aromatic), 1624m (CO), 1584m (CO), 1557s (CC), 1500s (CC), 1392vs (C–O), 1207s, 761vs, 717vs; ^{1}H NMR (300 MHz; DMSO-d_6) δ 9.50 (m, 2H), 8.59 (d, J = 7.77 Hz, 2H), 8.44–8.39 (m, 2H), 8.15–8.09 (m, 2H), 7.86–7.69 (m, 4H), 7.55–7.45 (m, 1H), 6.36 (d, J = 8.46 Hz, 1H) ppm; ^{13}C NMR (101 MHz, DMSO-d_6) δ 181.36, 173.83, 157.27, 156.30, 148.83, 140.95, 140.21, 134.05, 133.53, 133.01, 128.34, 128.13, 126.54, 126.24, 124.64, 123.00, 119.92 ppm; MS (ESI): m/z $[M]^+$ calcd 613.49; found 461.19 $[M - C_7H_4O_2]^+$.

[(L8)Pt(aliz)], 8b. The reaction conditions were analogous to those reported for **1b**. The reaction was conducted using **8a** (80 mg, 0.18 mmol), H_2(aliz) (43 mg, 0.18 mmol) and KOH (30 mg, 0.72 mmol). Black-purple solid, yield 51%; m.p. >250 °C; $C_{26}H_{14}N_2O_4Pt$ (MW = 613.48): Anal. calcd: C, 50.90; H, 2.30; N, 4.57%; found: C, 50.88; H, 2.33; N, 4.55%; FT-IR (KBr) ν(cm^{-1}) = 3082s (CH aromatic), 3059s (CH aromatic), 1626s (CO), 1585m (CO), 1492vs, 1462m (CC), 1382vs (C–O), 1208s, 839vs, 716m, 707vs; ^{1}H NMR (300 MHz; DMSO-d_6) δ 9.69 (d, J = 5.43 Hz, 2H), 9.04 (d, J = 7.77 Hz, 2H), 8.29 (s, 2H), 8.19–8.10 (m, 4H), 7.76–7.66 (m, 2H), 7.47 (d, J = 8.28 Hz, 1H), 6.29 (d, J = 8.52 Hz, 1H) ppm; ^{13}C NMR (101 MHz, DMSO-d_6) δ 198.48, 187.82, 174.37, 150.84, 149.84, 140.39, 139.47, 137.12, 134.38, 134.00, 132.87, 131.21, 128.61, 127.27, 126.97, 126.84, 126.72, 124.23, 123.42, 120.34, 118.45 ppm; MS(ESI): m/z $[M]^+$ calcd 613.49; found 469.25 $[M - C_8H_4O_3]^+$.

[(L9)Pt(aliz)], 9b. The reaction conditions were analogous to those reported for **1b**. The reaction was conducted using **9a** (80 mg, 0.16 mmol), H_2(aliz) (38 mg, 0.16 mmol) and KOH (36 mg, 0.64 mmol). Light purple solid, yield 57%; m.p. >250 °C; $C_{28}H_{14}N_4O_4Pt$ (MW = 665.52): Anal. calcd: C, 50.53; H, 2.12; N, 8.42%; found: C, 50.56; H, 2.09; N, 8.40%; FT-IR (KBr) ν(cm^{-1}) = 3122w (CH aromatic), 1624m (CO), 1584m

(CO), 1555s (CC), 1497vs, 1462vs, 1389vs (C–O), 1206s, 716s; ^{1}H NMR (300 MHz; DMSO-d_6) δ 9.47 (pseudo-dd, 1H), 9.25 (m, 1H), 9.17 (pseudo s, 2H), 8.15–8.09 (m, 2H), 7.97 (dd, 2H), 7.79–7.73 (m, 2H), 7.54 (d, J = 8.22 Hz, 1H), 6.42 (d, J = 8.76 Hz, 1H) ppm; ^{13}C NMR (101 MHz, DMSO-d_6) δ 188.48, 156.14, 152.92, 147.66, 146.28, 140.46, 136.41, 134.56, 134.40, 133.40, 132.83, 127.38, 126.87, 126.71, 125.23, 125.12, 120.78, 119.41, 115.22 ppm; MS(ESI): m/z $[M]^+$ calcd 665.53; found 591.91 $[M - C_6H_4]^+$.

Log P_{ow} determination

RP-HPLC analyses were performed to correlate the hydrophobicity of the platinum(II) complexes with their retention time. The chromatograms were registered using a Partisil C18-ODS reversed-phase HPLC column, at 25 °C and with a water/methanol ratio of 80/20 in the presence of 15 mM HCOOH as the mobile phase and using KI as the internal standard (flow rate of 1 mL min^{-1}, λ = 210 nm). The calibration curve was realized in comparison with reference compounds, chosen in commercially available platinum compound series (*i.e.* cisplatin, oxaliplatin and carboplatin).[24,25]

Interaction study with GSH

The binding studies with GSH were directly conducted in NMR tubes mixing 1 eq. of the compound (**2b**, **6b** or **7b**) in 20% of 0.9% w/v NaCl–D_2O solution in DMSO-d_6; then 1.1 eq. GSH was added to the solution. The sample was evaluated at 24 h by ^{1}H NMR analysis.

Cell culture

The breast cancer cell line MDA-MB-231 cells were cultured in DMEM supplemented with penicillin (10 000 U mL^{-1}), streptomycin (10 mg mL^{-1}), non-essential amino acid solution and 10% fetal calf serum (FCS). The cells were incubated with newly synthesized complexes dissolved in DMSO. The same volume of solvent was added to control conditions and did not exceed 0.5% v/v.[24,25]

Sulphorodamine B cell viability assay

Cellular toxicity of the MR compounds was assessed using the sulphorodamine (SRB) assay according to the protocol established by Skehan *et al.*[47] 8000 cells per well were seeded in a 96 well-tray in 100 µl per well of the complete medium. The following day, the medium was replaced with fresh media containing 0.4% FBS and treatments or DMSO as the control. After 24 h of incubation, the SRB assay was performed and absorbances were measured at 570 nm with a Victor Nivo multiplate reader by PerkinElmer.

Determination of intracellular and DNA-bound Pt concentrations

For the DNA-bound Pt concentrations, the nuclear DNA was extracted by incubating cell monolayers with digest buffer (final composition: 50 mM in Tris HCl, 100 mM NaCl, 100 mM EDTA, 1% SDS), then transferred to 1.5 mL microcentrifuge tubes and a saturated NaCl solution was added. The samples were then clarified by centrifugation for 15 min at 13 000 rpm and the supernatant transferred to new microcentrifuge tubes and DNA precipitated by isopropanol. DNA was then washed by centrifugation twice with 70% ethanol and resuspended in TE buffer (10 mM Tris pH 8.0, 0.1 mM EDTA). The Pt concentrations were then determined by ICP-MS and normalized by total DNA. For the determination of total intracellular Pt concentrations, cells were washed twice with PBS and lysed by incubation with 1% Triton X100/0.1% SDS for 5 min at room temperature. Cell lysates were then removed by centrifugation at 14 000*g* for 10 min, and the Pt concentrations were determined by ICP-MS (the calibration curve was realized by using platinum chloride standard solution (platinum standard solution, for AAS, 1 mL = 1.00 mg Pt = 5.13 mmol L^{-1} in 10–20% HCl)). Data were normalized with the protein concentrations determined using the BCA protein assay (Thermo Scientific, Rockford, IL USA).

ESI MS experiments

Sample preparation: stock solutions of ODN (Merck), bovine pancreatic ribonuclease A (Merck) and human serum albumin (Merck) 10^{-3} M were prepared by dissolving the lyophilized protein or oligonucleotide in LC-MS grade water. Stock solutions of 10^{-2} M platinum compounds were prepared by dissolving the samples in acetonitrile. For the experiments, an aliquot of the stock solutions of the selected protein was mixed with aliquots of each platinum compound at a protein-to-metal ratio of 1 : 1 and diluted with 2 mM ammonium acetate solution (pH 6.8) to 100 µM final protein concentration. The mixtures were incubated at 37 °C up to 48 h. After the incubation time, the protein solutions were sampled and diluted to a final protein concentration of 500 nM using 2 mM ammonium acetate solution, pH 6.8 and adding 0.1% v/v formic acid just before the infusion in the mass spectrometer. For the oligomer the final concentration was 1 µM, diluted with 2 mM ammonium acetate solution, pH 6.8 and 1% v/v triethylamine was added just before infusion in the mass spectrometer. Instrumental parameters: the ESI mass spectra were acquired through direct infusion at 7 µL min^{-1} flow rate in a Tri-pleTOF® 5600+ high-resolution mass spectrometer (Sciex, Framingham, MA, U.S.A.), equipped with a DuoSpray® interface operating with an ESI probe.

The ESI source parameters were as follows:

RNase: positive polarity, ionspray voltage floating 5500 V, temperature 0, ion source gas 1 (GS1) 45 L min^{-1}; ion source gas 2 (GS2) 0; curtain gas (CUR) 15 L min^{-1}, declustering potential (DP) 60 V, collision energy (CE) 10 V, acquisition range 570–1300 m/z.

HSA: positive polarity, ionspray voltage floating 5500 V, temperature 0, ion source gas 1 (GS1) 30 L min^{-1}; ion source gas 2 (GS2) 0; curtain gas (CUR) 12 L min^{-1}, declustering potential (DP) 150 V, collision energy (CE) 10 V, acquisition range 1000–2600 m/z.

ODN: negative polarity, ionspray voltage floating −4500 V, temperature 0, ion source gas 1 (GS1) 30 L min^{-1}; ion source gas 2 (GS2) 0; curtain gas (CUR) 20 L min^{-1}, declustering

potential (DP) 50 V, collision energy (CE) 10 V, acquisition range 600–1400 *m*/*z*.

For acquisition, Analyst TF software 1.7.1 (Sciex) was used, and deconvoluted spectra were obtained by using the Bio Tool Kit micro-application v.2.2 embedded in Peak-ViewTM software v.2.2 (Sciex).

Theoretical calculations

All the quantum mechanical calculations were performed using density functional theory (DFT) by using the Gaussian16 software package.[48] The hybrid B3LYP exchange and correlation functional,[49,50] comprised of Grimme's dispersion correction (D3), was used for the optimization calculations in conjunction with the Pople double-ζ basis set 6-31+G* for the oxygen atoms and 6-31G** for C, N and H atoms; while the effective core potentials (ecp) SDD[51,52] were used for the Pt atom along with the associated split valence basis set. The aqueous environment effects were taken into consideration by the integral equation formalism variant of the polarizable continuum model (IEFPCM),[53] using a dielectric constant of 78.4. Harmonic frequency calculations were performed in order to identify both the minimum and transition state nature of each stationary point (0 or 1 imaginary vibrational frequencies, respectively) and to get Gibbs free energies at 298 K and 1 atm from total energies, including zero-point, thermal and solvent corrections.[54] Intrinsic reaction coordinate analysis was performed to properly connect minima to each transition state.[55,56] Final energies were obtained by means of single-point calculations employing the triple-ζ basis set 6-311+G** for all the atoms, except Pt for which ECP def2-QZVP basis set was employed in conjunction with the split valence basis set. UV–Vis spectra were achieved, within the non-equilibrium time dependent (TD) DFT approach, as vertical electronic excitations on the ground-state structure, using the same protocol as that used for the optimization calculations.

The gauge-independent atomic orbital (GIAO) method[57,58] was used to estimate the absolute chemical shielding as implemented in Gaussian 16. The standard basis set 6-311++G** for all the atoms and the SDD for the Pt center, were coupled to the B3LYP functional. Chemical shifts have been then obtained from absolute shieldings by subtraction of a calculated reference, the absolute chemical shielding of TMS computed at the same level of theory.

Results and discussion

Synthesis and characterization

Complexes [(N^N)Pt(aliz)], **1b–9b** were prepared starting from their corresponding [(N^N)$PtCl_2$] precursors, **1a–9a**, obtained following or adapting already reported procedures,[40–43] to afford after filtration and washing the desired products in overall good yields of 60–90% (Scheme 1).

All complexes were obtained as dark powders, mostly insoluble in the common organic solvents except for dimethyl sulfoxide (DMSO). Complexes **1b–9b** were fully characterized through spectroscopic characterization (FT-IR, multinuclear NMR, and electrospray ionization ESI-MS) as well as melting point determination and elemental analysis. In the free H_2(aliz) ligand, the (C═O) bands are present at 1683 and 1663 cm^{-1} while the (C–O) band is at 1320 cm^{-1}.[22,59] In complexes **1b–9b**, the (C═O) stretching vibration band is present as a red-shifted medium or a strong band centred at 1625 cm^{-1}. Moreover, each spectrum exhibits an intense band at *ca.* 1555 cm^{-1} that can be reconducted to mixed (C═O) and (C═C) vibrations. With regards to the C–O bond, a very strong absorption band is present at 1349 cm^{-1} for **1b** and in the range of 1382–1392 cm^{-1} for complexes **2b–9b**. Lastly, for the complexes **1b–6b**, it is important to underline the presence of the stretching bands related to the (N–H) vibrations. Specifically, they are positioned at 3303–3200 (**1b**), 3219 (**2b**), 3224 (**3b**), 3486 (**4b**), 3522 cm^{-1} (**5b**) and 3367 (**6b**) cm^{-1}, respectively. ^{1}H NMR spectra confirm exhaustively once again the complexation of aliz. For each complex **1b–9b** the coordination of aliz is testified by the shift of the aliz protons nearest to coordination sites, the most sensitive protons to ligand coordination. In each spectrum, the signal of the two H most sensitive to metal coordination is shifted to high fields with respect to H_2(aliz) and, in particular, of *ca*. 0.72 and 0.10 ppm respectively. Notably, the synthesis of complexes **3b–6b** could afford a mixture of geometrical isomers, due to the asymmetry of both aliz and their corresponding (N^N) ligand.[60] The *cis*/*trans* isomers can be

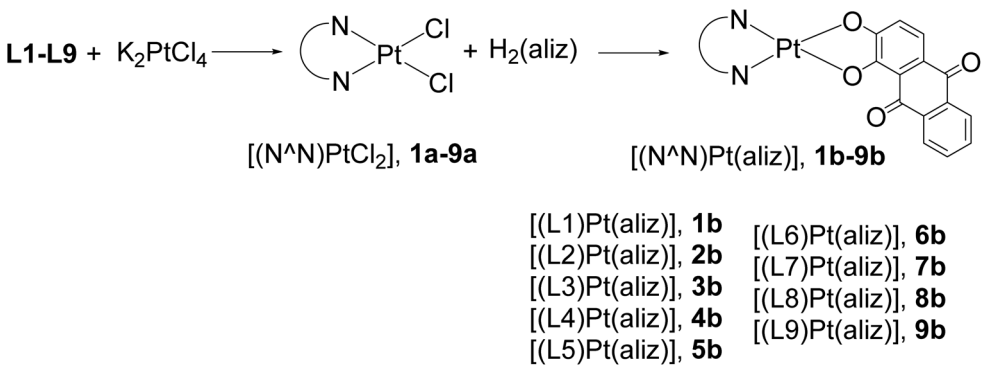

Scheme 1 Synthesis of [(N^N)$Pt(aliz)_2$] complexes, **1b–9b**.

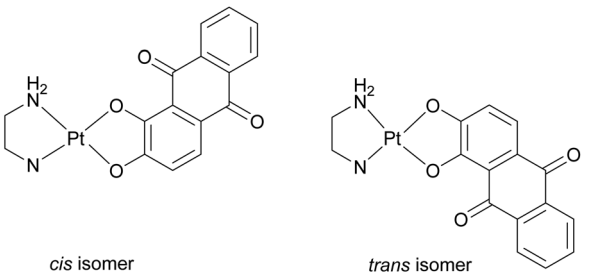

Fig. 3 Geometric *cis*/*trans* isomers of complexes **3b–6b**.

defined in function of the relative position of the N-atom of the $-NH_2$ function with respect to the more sterically hindered O-chelated atom of the alizarin ligand (Fig. 3).

However, the ^{1}H NMR spectra of compounds **3b–6b** display a sole set of signals for both ligands evidencing that only a single isomer was obtained in each case. The spectral features of the two possible isomers of complexes **3b–6b** were simulated in the framework of the GIAO method in order to establish if there is any evidence supporting the presence of one or other isomers in the examined sample. Both ^{13}C and ^{1}H NMR spectrum simulations of the two possible isomers of complexes **3b–6b** evidenced a very similar behavior of the two species; no significant difference in the computed chemical shifts (collected in Table S1†) about the key region of each complex was found. Even from a thermodynamic point of view, the relative stability of the two isomers differs by no more than 0.5 kcal mol^{-1}. In the absence of suitable crystals for X-Ray diffraction, to shed light on the nature of the synthesized isomer, we computationally analyzed the shortest distances between protons of the two ligands separated by the Pt (II) metal center in the complexes, looking for possible candidates prone to display the nuclear Overhauser effects (NOE). Measured distances computed in DMSO were extracted from the optimized geometries of complexes **3b–6b** as reported in Table TS2.† Comparing the interproton distances complex **5b** with a methyl group at the *ortho*-position of the pyridine ring has been identified as the rightful candidate for this study. Indeed, the interproton distance between the protons of the methyl group and the nearest proton of the alizarin ligand is 3.85 Å in the *cis* isomer, an ideal value for a NOE effect, as observed in the case of a Pd(II) complex.[61] Therefore, in a 2D-NOESY experiment, it is expected that *cis*-**5b** isomer is expected to display two correlations: one with the nearest proton of alizarin, and one with the neighboring proton of the pyridine ring, while the *trans*-**5b** isomer should only display the latter one. The 2D-NOESY spectrum of **5b** recorded in DMSO-d_6 as reported in Fig. S16,† clearly shows a unique NOE effect, thus evidencing that the *trans* isomer was produced. It is therefore hypothesized that for all complexes **3b–6b**, only the *trans* isomer was indeed synthesized.

From a structural point of view, computations evidenced that all the complexes are characterized by a square planar structure in which the O^O and the N^N ligands, when fully aromatic, are coplanar to each other. While a distortion from the planarity on the N^N ligand can be observed, as expected, when one or both nitrogen atoms coordinated to the platinum center are sp^3. The nature of the N^N ligands has only a marginal influence on the Pt–N and Pt–O bond lengths, as previously reported for some aquo complexes with similar nitrogen ligands.[32] However, looking at such distances reported in Fig. S17† a slight shortening of the Pt–O bond *trans* to aromatic N as compared to *trans* to NH_2 can be observed. Similarly, the Pt–N distances involving aromatic nitrogen atoms are shorter than those with non-aromatic ones. For further detailed description, cartesian coordinates are reported in Table TS3.†

Stability of Pt complexes in buffered solutions (experimental and theoretical)

The UV–Visible absorption spectra of complexes **1b–9b** were recorded in 1×10^{-5} M DMSO/buffer solution (DMSO 0.5% v/v) at room temperature, and the results are shown in Fig. 4. Moreover, in order to spectroscopically assess the long-term stability of all compounds in an aqueous medium, the absorption profiles were acquired over time (0, 3, 6 and 24 h) (Fig. S18†). The TD-DFT computed spectra in the water environment are reported in Fig. S19† and more detailed information collected in Table S4.† Both aqueous solutions of **1b** and **2b**, bearing N^N ligands **L1** and **L2**, respectively, display

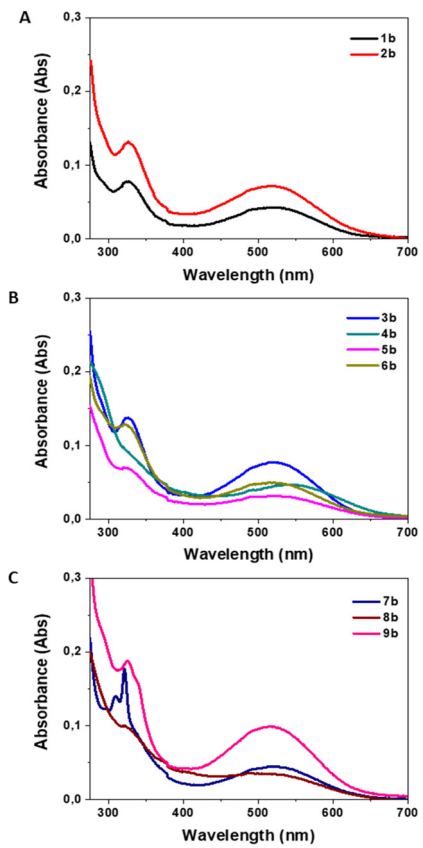

Fig. 4 Absorption spectra of complexes **1b–2b** (A), **3b–6b** (B), and **7b–9b** (C).

absorption spectra characterized by a peak at 326 nm and by a broad, structureless electronic band at a lower energy (440–650 nm). In agreement with the experimental and theoretical absorption spectra of the analogous compound [$(NH_3)_2$Pt(aliz)] and other aliz transition metal complexes[25,62–64] such a band is assigned to metal to ligand charge-transfer (MLCT) transitions involving the aliz fragment (Fig. 4A). Indeed, the plot of the natural transition orbitals (NTOs), reported in Fig. S20,† confirm the MLCT nature of the band, which is generated by a pure electronic transition from HOMO to LUMO centered at 517 and 513 nm for **1b** and **2b**, respectively. The highest energy peak, is, instead, due to an intraligand charge transfer localized on the aliz ligand (ILCT), with a very weak participation of the metal only in the case of **1b**. The electronic transition starts from an inner orbital (H-4) and ends at the LUMO.

Analogously **3b–6b**, all characterized by having a sp^2 hybridized nitrogen atom in the coordination sphere, show electronic absorption features in the UV–Visible range very similar to those of the related [$(NH_3)_2$Pt(aliz)] complex, pointing out the predominant involvement of the (O^O) ligand over the (N^N) one (Fig. 4B). The two bands, thus, originated by transitions with MLCT and ILCT character in the regions 440–650 and 275–420 nm, respectively.

The recorded and computed absorption spectra of the Pt(II)-diamine complexes **7b–9b** are reported in Fig. 4C and Fig. S19C.† In all cases, a band between 440 and 650 nm is observed, attributed to a charge-transfer transition from the metal center to the aliz ligand. Nevertheless, differently from the other cases, the plot of NTOs clearly proves the participation of the (O^O) ligand in the charge transfer from the metal center (Fig. S20†). In the highest energy region (275–420 nm), also according to the comparison with the absorption spectra of the representative Pt(II) complexes **7a–9a**, **7b–9b** exhibit bands attributable to MLCT transitions involving the (O^O) ligand as well as the (N^N) ligand.[65,66] This is particularly evident in the case of **9b**, for which a contribution of transitions having ligand to ligand charge transfer character can be highlighted.

In conclusion, it is possible to state that the photophysics of compounds **1b–9b** is characterized by electronic transitions which strongly involve the 1,2-dihydroxy-9,10-anthraquinone ligand, as also observed in other alizarin-bearing coordination compounds.[67,68]

Log P_{ow} and pharmacological evaluation

For complexes **1b–9b**, log P_{ow} values were determined by RP-HPLC and using commercially available Pt(II) complexes as references.[69–71] The values were generally comparable, in a range of 2.79–3.57, depending on the type of the N^N ligands and on the presence of aliz (Table 1 and Fig. S13–15†).

The cytotoxicity of complexes **1b–9b** was tested *in vitro* on a triple negative breast cancer MDA-MB-231 cell line by the sulforhodamine B (SRB) assay. After 24 h incubation with increasing concentrations of the compounds, the IC_{50} values were determined. As shown in Table 1, by the analysis of the cytotoxic activity results, only **5b**, **6b** and **7b** showed a considerable decrease of cell viability with IC_{50} values of 89.54 ± 2.21 μM (**5b**), 10.49 ± 1.21 μM, (**6b**) and 24.5 ± 1.5 μM (**7b**), respectively. In particular, **6b** revealed the lowest IC_{50} value.

Table 1 Log P_{ow} and cytotoxic effects of **1b–9b** complexes on MDA-MB-231

[(N^N)Pt(aliz)] complexes	Log P_{ow}[a]	IC50 on MDA-MB-231[b]
1b	2.84	>200 μM
2b	2.82	>200 μM
3b	2.87	>200 μM
4b	3.26	>200 μM
5b	3.57	89.54 ± 2.21 μM
6b	3.39	10.49 ± 1.21 μM
7b	2.81	24.5 ± 1.5 μM
8b	2.79	>200 μM
9b	2.79	>200 μM
Cisplatin	-2.21	59.4 ± 10.06 μM

[a] Log P_{ow} was evaluated by RP-HPLC, equipped with C18 ODS at 25 °C with water/methanol in ratio 80/20 in presence of 15 mM HCOOH as an eluent. [b] IC_{50} values were determined by the sulforhodamine B (SRB) assay.

Given the promising values of cytotoxicity obtained for some of the complexes, the object of this work, the intent was to study their possible mechanism of action. Therefore, we decided to deeply investigate complexes **2b**, **6b** and **7b** which are similar from the structural point of view, but with very different cytotoxic profiles (not effective, 10.49 ± 1.21 μM and 24.5 ± 1.5 μM, respectively), in order to elucidate the fundamental role played by the (N^N) ligand. Furthermore, for a better understanding of the contribution of aliz in these three complexes' reactivity, they are compared to their dichloride precursors **2a** (IC_{50} value of 6.65 μM), **6a** (4.5 μM)[24] and **7a** (11.92 μM). In order to understand the cause of the difference in terms of activity of these six complexes, Pt(II) bioavailability was analyzed by measuring the intracellular concentrations of Pt concentrations by ICP-MS of cellular lysates. Surprisingly, we detected minimal amounts of Pt after 6 h of incubation with **6b** and **7b**. Instead, **2b**, **2a**, **6a** and **7a** produced the highest incorporation into cellular proteins (Fig. 5).

Since it was observed that the Pt established a minimal association with intracellular proteins, the amount of Pt bound to DNA was determined in order to justify its cytotoxic effect. The complex that displayed the largest affinity to nuclear DNA is **6b**, probably due to its efficient transport into the nucleus without affecting cellular proteins. The Pt percentage bound to DNA, in relation to the entire compound incubated, exhibited by **6b** was the highest compared to the other complexes selected. These results suggest that **6b** elicits its highly potent cytotoxic effect by a very large association with nuclear DNA with a minimal interaction with intracellular proteins. The DNA binding capacity of **6b** was significantly higher than cisplatin (Fig. 6).

ESI-MS and NMR interaction studies of Pt complexes with biological molecules

A number of binding studies were conducted according to a well-defined ESI-MS experimental protocol that was recently

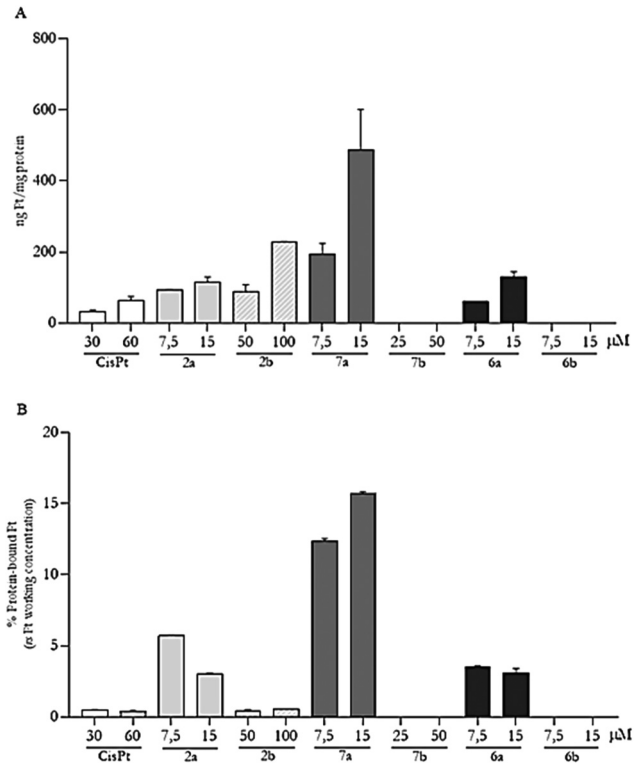

Fig. 5 Protein-bound concentrations of Pt after incubation of the MDA-MB-231 cell line with Pt(II) complexes. Cells were seeded (250 000/35 mm Petri dish) and incubated with DMEM supplemented with 10% FCS; 24 h later the medium was replaced with the one containing 0.4% FCS and indicated concentrations of compounds. The incubation was continued for 6 h at 37 °C. At the end of this incubation period, the total cell homogenates were prepared. (A) ng Pt per mg protein and (B) percentage of Pt protein-bound compared to μM concentration utilized.

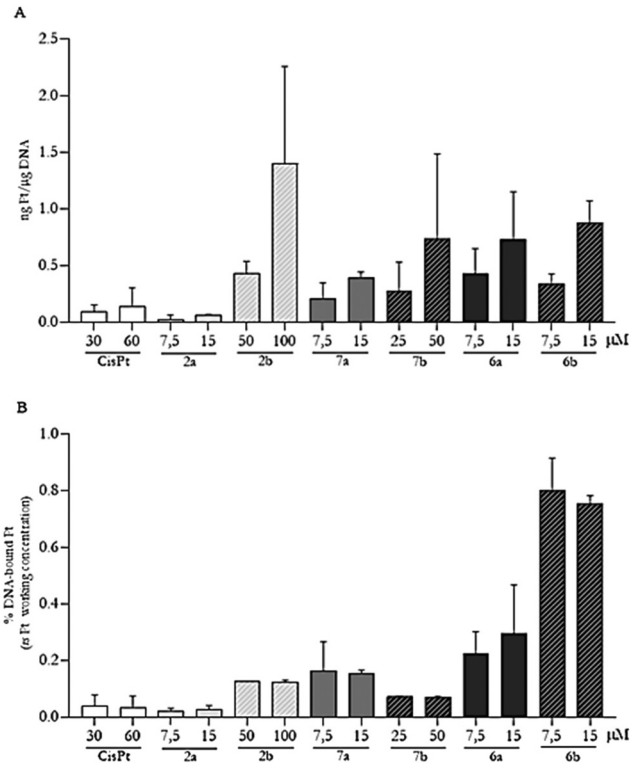

Fig. 6 DNA-bound concentrations of Pt after incubation of the MDA-MB-231 cell line with Pt(II) complexes and cisplatin. Cells were seeded (250 000/35 mm Petri dish) and incubated with DMEM supplemented with 10% FCS; 24 h later the medium was replaced with one containing 0.4% FCS and indicated concentrations of compounds. The incubation was continued for 6 h at 37 °C. At the end of this incubation period, the total DNA was extracted. (A) ng Pt per mg DNA and (B) percentage of Pt DNA-bound compared to μM concentration utilized.

developed in the METMED laboratory in Florence and is now documented in several papers.[72–74] In more detail, we reacted two distinct proteins, *i.e.* ribonuclease A (RNase A) and human serum albumin (HSA), and a DNA oligonucleotide, *i.e.* the single-stranded 12-mer ODN1, with equimolar amounts of three complexes **2b**, **6b** and **7b** and of their respective chloride counterparts (**2a**, **6a** and **7a**) and analyzed through ESI-MS the products of those interactions. Notably, HSA (65 kDa) is a relatively big globular protein characterized by the presence of 17 disulfide bonds and only one free cysteine residue (Cys34);[75] HSA is the most abundant protein in the plasma and is known to interact with several metallodrugs including the classical anticancer drug cisplatin.[76] RNase A (14 kDa) is a relatively small protein with four disulfide bonds in its native state, *i.e.*, Cys26–84, Cys58–110, Cys40–95 and Cys65–72; these disulphide bonds are relatively well exposed to the solvent. RNase is usually used as a model protein to better understand the molecular mechanisms of interaction of platinum metal complexes with proteins.[77] The DNA oligonucleotide ODN1 contains a single "GG" box in the middle of the sequence (5′-ATTAGGCCTAAT-3′) which is the typical binding site for the Pt(II) complexes.

Interestingly, the obtained ESI-MS spectra reveal a large difference in the reactivity of complex **6b** compared to **2b** and **7b**, despite their close structural relationship. Indeed, in the case of complex **6b**, an appreciable reactivity is observed with RNase and ODN1; in both cases complex **6b** leads to the formation of a well-defined adduct bearing the Pt(II) 8-aminoquinoline fragment (Fig. 7).

Conversely, complexes **2b** and **7b** did not show any significant reactivity with RNase and ODN1; no adduct formation was indeed detected in the ESI-MS spectra after incubation (data not shown). No adduct formation was detected between complexes **2b**, **6b** and **7b** and HSA.

At variance, all the chloride compounds, *i.e.* complexes **2a**, **6a** and **7a**, manifested a large reactivity towards all tested targets (RNase, HSA and ODN), owing to the presence of the more labile chloride ligands. In Fig. 7, the ESI-MS spectra of complex **6b** and its chloride counterpart, *i.e.* complex **6a**, interacting with the above biomolecules are comparatively shown. In all spectra the signal of the native biomolecule is retained indicating that complete metalation of the targets has not occurred. In the case of ODN1 the peak at 3643 Da belongs to the native oligonucleotide and the other two signals at 3980

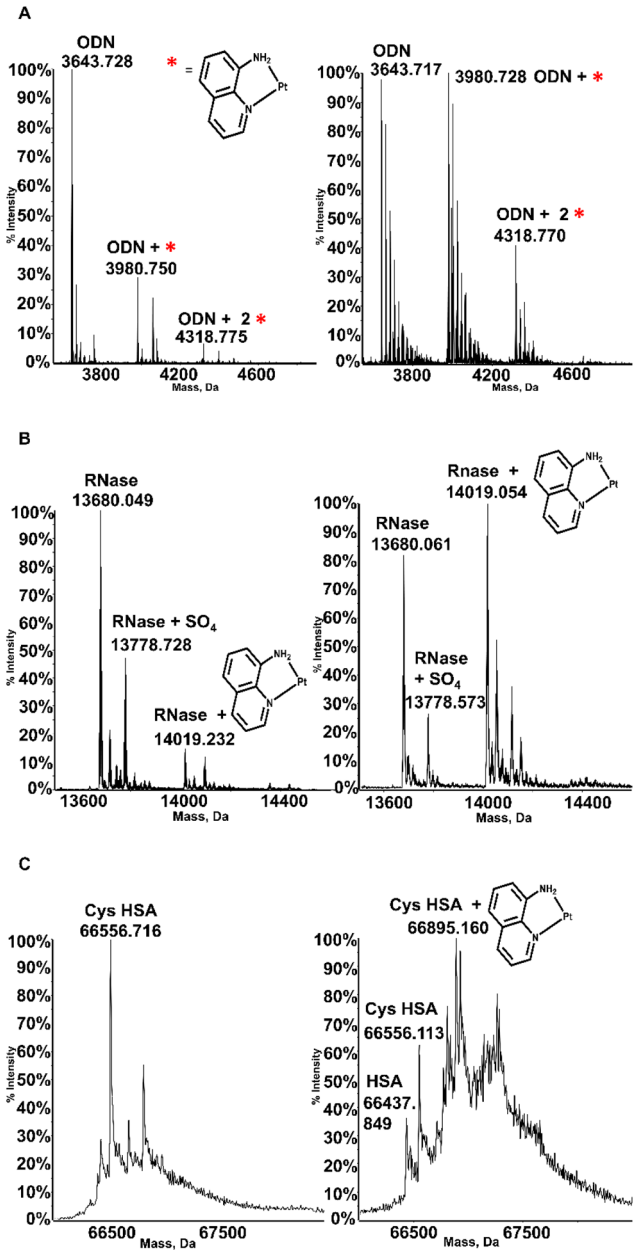

Fig. 7 (A) Deconvoluted ESI-Q-TOF spectra of ODN with complex **6b** (left) and **6a** (right). (B) Deconvoluted ESI-Q-TOF spectra of RNase with complex **6b** (left) and **6a** (right). (C) Deconvoluted ESI-Q-TOF spectra of HSA with complex **6b** (left) and **6a** (right), in a 1 : 1 molecules to platinum ratio. All spectra were recorded at 24 h.

Da and 4318 Da belong to the adducts with the Pt(II) 8-aminoquinoline fragment with a binding stoichiometry of up to 1 : 2 of metal fragment/target. A similar reaction pattern is also identified in the case of RNase, with the native protein signal at 13 680 Da and a binding stoichiometry of up to 1 : 1. Instead, complex **6b** did not react with HSA, as shown in Fig. 7C, while the complex **6a** interacts with the protein, binding the classical Pt(II) 8-aminoquinoline fragment.

These findings pointed out that the chloride leaving group enhanced the reactivity of the Pt(II) complexes compared to the aliz analogues. This aspect is also confirmed by the comparative studies performed with the well-known anticancer agent cisplatin. The interactions between this drug and some biological targets, such as ODN, RNase and HSA, were evaluated; the adduct formation with the metal fragment $[Pt(NH_3)^{2+}]$ was observed in the case of RNase and ODN (see Fig. S21†).

It turns out that the aliz ligand greatly reduced the ability of the Pt(II) complexes to interact with the model biomolecules. However, the greater reactivity of complex **6b** towards the targets, in contrast to the behavior of complexes **2b** and **7b**, was in good agreement with the cytotoxicity data; in fact, the cytotoxic data demonstrated that complex **6b** (IC_{50} value of 10.49 μM) was more active against the MDA-MB-231 cell line than complexes **2b** and **7b**, with IC_{50} values of >200 μM and 24.5 μM, respectively.

Regarding the interaction with GSH, an NMR study was performed (Fig. S22†). As shown in the ^{1}H NMR spectrum, the appearance of two multiplets at 3.1–3.3 and 2.8–2.95 ppm is noted, assigned to the shift of the methylene protons next to the SH group originally present as a multiplet located at 2.60–2.85 ppm. Moreover, the new multiplet at 4.55–4.70 ppm arose in the spectrum originally represented as a multiplet at 4.3–4.4 ppm and relative to two methane functions, underlining the interaction between the complexes and GSH, more evident after 24 h in the case of **6b**. With these types of complexes, despite the protective role possibly played by the aliz ligand, evidence is clearly obtained for sulfur coordination to the platinum center and adduct formation. Yet, it remains to be established to what extent the reaction proceeds in the real cellular environment and what is the precise platinum speciation. The relevant cytotoxic effects still produced by **6b** in cancer cells suggest that only partial inactivation of the platinum complex by GSH has occurred.

Computational exploration of the mechanism of action

Given the substantially different abilities of the characterized complexes in causing cell death, a detailed computational study was carried out to explore their respective mechanisms of action. On the basis of the measured IC_{50} (Table 1), complexes **2b**, **6b** and **7b** were selected as they can be considered as a representative of inactive, highly active and medium active complexes, respectively. For the sake of comparison, the same calculations were performed on the chlorido derivatives **2a**, **6a** and **7a**, the precursors of the selected complexes, in order to assess the influence of the aliz ligand on the anticancer action.

The key steps of the mechanism of action of Pt(II)-based anticancer drugs inside the cell, as depicted in Scheme 2, are as follows: (i) the labile ligand substitution by water molecules that leads to the formation of the corresponding aqua-complexes (hydrolysis) and (ii) the subsequent binding to nuclear DNA (DNA platination). The product of the first part of the mechanism can be both the mono- and di-aquo complexes as a result of the first and the second hydrolysis, respectively. Accordingly, the second part of the mechanism of action, that is DNA platination, can in principle involve either the mono-

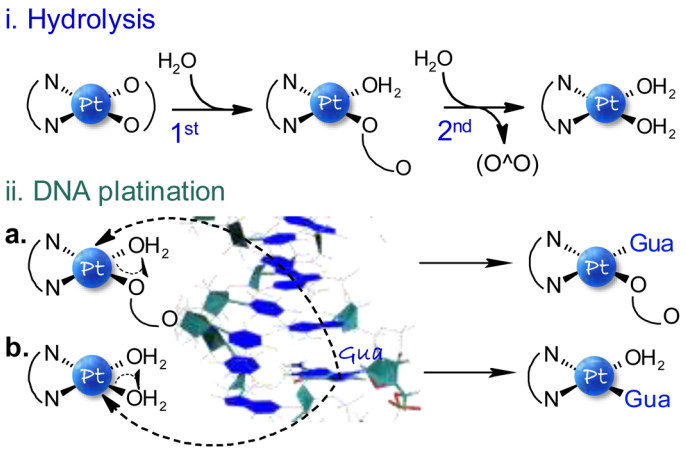

Scheme 2 Schematic reaction mechanism accounting for the mode of action of the anticancer [(N^N)Pt(aliz)] complexes.

aquo (path a) or the di-aquo complexes (path b). The latter step, as is well-known, causes the structural distortion of DNA that ultimately leads to cell death. Complex **6b**, as some of the investigated complexes for which the N^N ligand is not symmetric, can exist in two different isomeric forms. Calculations evidenced equal stability (energy difference of less than 0.5 kcal mol^{-1}) of the two isomers and, as no *trans* effect can influence the water attack, the anticancer activity was explored only for the *trans* isomer, being the experimentally obtained one.

In Table 2 the activation free energies and the reaction free energies computed for both hydrolysis steps and DNA platination, are reported.

The anticancer action starts with the entrance of water in place of one arm of the O^O ligand (1st hydrolysis). All the investigated complexes show approximately the same tendency to undergo the first hydrolysis. In all cases the reaction is endergonic in a range between 6 (for **6a**) and 17 kcal mol^{-1} (for **7b**). The detachment of one oxygen coordinating atom of aliz in favor of water coordination requires the highest energy amount to be realized in complex **2b** (see $\Delta G^{\ddagger}$ for the 1st hydrolysis in Table 2), while for the reference complex **6a** the lowest energy barrier was computed. The subsequent step, that is the formation of the diaquo-complex (2nd hydrolysis), is only slightly endergonic for all the complexes. The kinetics of the second hydrolysis is rather similar for all the complexes. The associated activation energies remain in a range of 20–23 kcal mol^{-1}. The energies put into play suggest the first hydrolysis as the rate limiting step of the complete aquation reaction, as found for the analogue neutral complex [$(NH_3)_2$Pt(aliz)] previously studied.[25]

DNA platination involves the attack of the Pt-based complexes to DNA nucleobases to form inter- and intrastrand crosslinks that cause structural distortion. Such a step of the anticancer action is usually modelled by simulating the attack on the preferred site of attack that is the guanine purine base of DNA at the N7 position.[78] Displacement of water allows guanine coordination to the metal center. This reaction was explored by taking into consideration the guanine attack to both mono- and di-aquo complexes (aGua and bGua in Table 2, respectively). The outcomes, in terms of activation and reaction free energies (Table 2), suggest that the behavior of the mono- and di-aquo complexes is similar for all the investigated complexes. Overall, the platination reaction is rather exergonic, similar to that observed for analogous complexes having the (C^N) ligand.[25,79]

The soft nature of the platinum center may result in deactivation of the complexes due to the presence in the biological environment of sulfur-containing molecules, which can form stable adducts with Pt(II) complexes. As in our previous works, *N*-acetyl methionine (NAM) was used as a representative of such a class of biological residues, with the aim to explore the proclivity of the investigated complexes to undergo the attack of sulphur-containing units.[80] The computed free energy profiles are reported in Fig. S23.† Outcomes evidence that complexes **2b** and **7b** exhibit the same reactivity toward NAM. In contrast, complex **6b** shows a certain resistance to being attacked by NAM. Among the chlorido derivatives, again, that bearing the L6 N^N ligand (**7a**) is less prone to undergo one aliz arm detachment in favor of NAM coordination. The adduct formation with NAM is endergonic in all cases, with the exception of **2a** and **6a** chlorido derivatives for which product stabilization, by about 2 and 6 kcal mol^{-1}, respectively was observed.

Table 2 Calculated activation ($\Delta G^{\ddagger}$) and reaction (ΔG_r) free energies (kcal mol^{-1}) in water describing the first and second hydrolysis processes and guanine interaction with mono- (*aGua*) and di-aquo (*bGua*) complexes

	1st		2nd		aGua		bGua	
	$\Delta G^{\ddagger}$	ΔG_r	$\Delta G^{\ddagger}$	ΔG_r	$\Delta G^{\ddagger}$	ΔG_r	$\Delta G^{\ddagger}$	ΔG_r
2b	28.0	10.7	22.8	6.2	17.8	−11.9	16.9	−12.4
6b	26.4	14.9	20.9	5.5	19.6	−14.2	13.1	−11.3
7b	23.1	16.3	21.2	4.9	19.5	−7.8	17.5	−15.9
2a	23.2	5.9	20.5	7.0	16.7	−10.6	—	—
6a	23.9	6.1	23.2	8.2	15.3	−15.1	—	—
7a	20.9	5.8	25.5	9.6	18.9	−11.5	—	—

Conclusions

In the herein proposed series of neutral mixed-ligand Pt(II) complexes, the bidentate ligand alizarin was rationally introduced as the leaving group with the idea of protecting the active Pt centre from the deactivation processes commonly occurring in cells. After a careful evaluation of their structural properties and their cytotoxic activities, three compounds, *i.e.*, **2b**, **6b** and **7b**, were chosen to understand in more detail the role of aliz in serving as a selective carrier of the Pt centre to nuclear DNA, the main target of these types of complexes.

Typically, these tetracoordinated Pt(II) complexes contain two bidentate ligands, *i.e.*, an inert ligand providing two nitrogen donors and aliz providing two oxygen donors. We noticed that the inert ligand can modulate importantly the biological activity of these Pt complexes. Indeed, only in two cases, *i.e.*, **6b** and **7b**, a significant cytotoxic activity was observed while the other Pt complexes turned out to be poorly active or inactive. The comparison of **2b**, **6b** and **7b** with their corresponding dichloride precursors **2a**, **6a** and **7a** is particularly instructive. Indeed, replacement of the two chloride ligands with aliz makes these compounds far more selective for DNA than for proteins; this is particularly true in the case of compounds **6b** and **7b** as clearly indicated by the ICP results. This feature makes aliz a very attractive ligand for the preparation of medicinal Pt complexes. ESI-MS and NMR interaction studies nicely supported the lower reactivity with targets of the aliz Pt complexes in comparison with their dichlorido analogues. The computational studies confirmed this possible mechanism of action, leading to the identification of the Pt(II) complex **6b** as a valid candidate for further pharmacological investigation.

Author contributions

R.C. and L.M.: data curation, investigation, and formal analysis. I.R. and G.C.: data curation, formal analysis, and investigation. L.R.: data curation and formal analysis, G.F.: validation and writing – review & editing. A.G. and M.G.L.: data curation and formal analysis. M.M. and V.V.: data curation. L.R.: investigation, I.A.: supervision, investigation, writing – review & editing, and funding acquisition. N.G. and L.M.: data curation and resources. N.F.: investigation and data curation. G.M.: investigation, data curation, and writing – original draft. E.S.: data curation and formal analysis. I.R.: conceptualization, project administration, supervision, and writing – review & editing. All the authors have read and approved the final manuscript.

Conflicts of interest

There are no conflicts to declare.

Acknowledgements

The present work was partially financed by "Progetto STAR 2 (PIR01_00008)"- Italian Ministry of University and Research and by "Project Sviluppo di tecnologie di materiali e di tracciabilità per la sicurezza e la qualità dei cibi- Demetra (PON ARS01_00401)".

References

1 T. C. Johnstone, K. Suntharalingam and S. J. Lippard, The Next Generation of Platinum Drugs: Targeted Pt(II) Agents, Nanoparticle Delivery, and Pt(IV) Prodrugs, *Chem. Rev.*, 2016, **116**(5), 3436–3486, DOI: **10.1021/acs.chemrev.5b00597**.

2 G. Facchetti and I. Rimoldi, Anticancer platinum(II) complexes bearing N-heterocycle rings, *Bioorg. Med. Chem. Lett.*, 2019, **29**(11), 1257–1263, DOI: **10.1016/j.bmcl.2019.03.045**.

3 G. Coffetti, M. Moraschi, G. Facchetti and I. Rimoldi, The Challenging Treatment of Cisplatin-Resistant Tumors: State of the Art and Future Perspectives, *Molecules*, 2023, **28**(8), 3407.

4 S. Rottenberg, C. Disler and P. Perego, The rediscovery of platinum-based cancer therapy, *Nat. Rev. Cancer*, 2021, **21**(1), 37–50, DOI: **10.1038/s41568-020-00308-y**.

5 N. J. Wheate, S. Walker, G. E. Craig and R. Oun, The status of platinum anticancer drugs in the clinic and in clinical trials, *Dalton Trans.*, 2010, **39**(35), 8113–8127, DOI: **10.1039/C0DT00292E**.

6 S. Ghosh, Cisplatin: The first metal based anticancer drug, *Bioorg. Chem.*, 2019, **88**, 102925, DOI: **10.1016/j.bioorg.2019.102925**.

7 J. Zhou, Y. Kang, L. Chen, H. Wang, J. Liu, S. Zeng and L. Yu, The Drug-Resistance Mechanisms of Five Platinum-Based Antitumor Agents, *Front. Pharmacol.*, 2020, **11**, 343, DOI: **10.3389/fphar.2020.00343**.

8 J. D. Monroe, H. L. Hruska, H. K. Ruggles, K. M. Williams and M. E. Smith, Anti-cancer characteristics and ototoxicity of platinum(II) amine complexes with only one leaving ligand, *PLoS One*, 2018, **13**(3), e0192505, DOI: **10.1371/journal.pone.0192505**.

9 M.-X. Tan, Z.-F. Wang, Q.-P. Qin, B.-Q. Zou and H. Liang, Complexes of oxoplatin with rhein and ferulic acid ligands as platinum(IV) prodrugs with high anti-tumor activity, *Dalton Trans.*, 2020, **49**(5), 1613–1619, DOI: **10.1039/C9DT04594E**.

10 F. Liu, X. Dong, Q. Shi, J. Chen and W. Su, Improving the anticancer activity of platinum(IV) prodrugs using a dual-targeting strategy with a dichloroacetate axial ligand, *RSC Adv.*, 2019, **9**(39), 22240–22247, DOI: **10.1039/C9RA03690C**.

11 P. Fronik, I. Poetsch, A. Kastner, T. Mendrina, S. Hager, K. Hohenwallner, H. Schueffl, D. Herndler-Brandstetter, G. Koellensperger, E. Rampler, *et al.*, Structure–Activity Relationships of Triple-Action Platinum(IV) Prodrugs with Albumin-Binding Properties and Immunomodulating

Ligands, *J. Med. Chem.*, 2021, **64**(16), 12132–12151, DOI: 10.1021/acs.jmedchem.1c00770.

12 A. D. Aputen, M. G. Elias, J. Gilbert, J. A. Sakoff, C. P. Gordon, K. F. Scott and J. R. Aldrich-Wright, Potent Chlorambucil-Platinum(IV) Prodrugs, *Int. J. Mol. Sci.*, 2022, **23**(18), 10471.

13 P. Fronik, M. Gutmann, P. Vician, M. Stojanovic, A. Kastner, P. Heffeter, C. Pirker, B. K. Keppler, W. Berger and C. R. Kowol, A platinum(IV) prodrug strategy to overcome glutathione-based oxaliplatin resistance, *Commun. Chem.*, 2022, **5**(1), 46, DOI: 10.1038/s42004-022-00661-z.

14 H. Shi, G. J. Clarkson and P. J. Sadler, Dual action photosensitive platinum(II) anticancer prodrugs with photoreleasable azide ligands, *Inorg. Chim. Acta*, 2019, **489**, 230–235, DOI: 10.1016/j.ica.2019.02.016.

15 K. Mitra, S. Gautam, P. Kondaiah and A. R. Chakravarty, Platinum(II) Complexes of Curcumin Showing Photocytotoxicity in Visible Light, *Eur. J. Inorg. Chem.*, 2017, **2017**(12), 1753–1763, DOI: 10.1002/ejic.201601078.

16 H. Mastalarz, A. Mastalarz, J. Wietrzyk, M. Milczarek, A. Kochel and A. Regiec, Synthesis of Platinum(II) Complexes with Some 1-Methylnitropyrazoles and In Vitro Research on Their Cytotoxic Activity, *Pharmaceuticals*, 2020, **13**(12), 433.

17 M. Sancho-Albero, G. Facchetti, N. Panini, M. Meroni, E. Bello, I. Rimoldi, M. Zucchetti, R. Frapolli and L. De Cola, Enhancing Pt(IV) complexes anticancer activity upon encapsulation in stimuli responsive nanocages, *Adv. Healthcare Mater.*, 2023, 1–12, DOI: 10.1002/adhm.202202932.

18 I. Rimoldi, V. Coccè, G. Facchetti, G. Alessandri, A. T. Brini, F. Sisto, E. Parati, L. Cavicchini, G. Lucchini, F. Petrella, *et al.*, Uptake-release by MSCs of a cationic platinum(II) complex active in vitro on human malignant cancer cell lines, *Biomed. Pharmacother.*, 2018, **108**, 111–118, DOI: 10.1016/j.biopha.2018.09.040.

19 M. Ghedini, A. Golemme, I. Aiello, N. Godbert, R. Termine, A. Crispini, M. La Deda, F. Lelj, M. Amati and S. Belviso, Liaisons between photoconductivity and molecular frame in organometallic Pd(ii) and Pt(ii) complexes, *J. Mater. Chem.*, 2011, **21**(35), 13434–13444, DOI: 10.1039/C1JM11926E.

20 A. Crispini, D. Pucci, I. Aiello and M. Ghedini, Synthesis and crystal structure of dinuclear cyclopalladated 1,2- and 1,3-bridged squarato complexes, *Inorg. Chim. Acta*, 2000, **304**(2), 219–223, DOI: 10.1016/S0020-1693(00)00091-8.

21 A. Ionescu, N. Godbert, I. Aiello, L. Ricciardi, M. La Deda, A. Crispini, E. Sicilia and M. Ghedini, Anionic cyclometalated Pt(ii) and Pt(iv) complexes respectively bearing one or two 1,2-benzenedithiolate ligands, *Dalton Trans.*, 2018, **47**(33), 11645–11657, DOI: 10.1039/C8DT02444H.

22 E. I. Szerb, A. Ionescu, N. Godbert, Y. J. Yadav, A. M. Talarico and M. Ghedini, Anionic cyclometallated iridium(III) complexes containing substituted bivalent ortho-hydroquinones, *Inorg. Chem. Commun.*, 2013, **37**, 80–83, DOI: 10.1016/j.inoche.2013.09.038.

23 A. Ionescu, R. Caligiuri, N. Godbert, L. Ricciardi, M. La Deda, M. Ghedini, N. Ferri, M. G. Lupo, G. Facchetti, I. Rimoldi, *et al.*, Cytotoxic performances of new anionic cyclometalated Pt(II) complexes bearing chelated O^O ligands, *Appl. Organomet. Chem.*, 2020, **34**(3), e5455, DOI: 10.1002/aoc.5455.

24 G. Facchetti, N. Ferri, M. G. Lupo, L. Giorgio and I. Rimoldi, Monofunctional PtII Complexes Based on 8-Aminoquinoline: Synthesis and Pharmacological Characterization, *Eur. J. Inorg. Chem.*, 2019, **2019**(29), 3389–3395, DOI: 10.1002/ejic.201900644.

25 G. Mazzone, S. Scoditti, R. Caligiuri, L. Ricciardi, E. Sicilia, M. G. Lupo, I. Rimoldi, N. Godbert, M. La Deda, A. Ionescu, *et al.*, Cytotoxicity of Alizarine versus Tetrabromocathecol Cyclometalated Pt(II) Theranostic Agents: A Combined Experimental and Computational Investigation, *Inorg. Chem.*, 2022, **61**(18), 7188–7200, DOI: 10.1021/acs.inorgchem.2c00842.

26 H. Liu, C. Zang, M. H. Fenner, K. Possinger and E. Elstner, PPARgamma ligands and ATRA inhibit the invasion of human breast cancer cells in vitro, *Breast Cancer Res. Treat.*, 2003, **79**(1), 63–74, DOI: 10.1023/a:1023366117157, From NLM.

27 K. J. Chavez, S. V. Garimella and S. Lipkowitz, Triple negative breast cancer cell lines: one tool in the search for better treatment of triple negative breast cancer, *Breast Dis.*, 2010, **32**(1–2), 35–48, DOI: 10.3233/bd-2010-0307, From NLM.

28 M. Maji, S. Karmakar, Ruturaj, A. Gupta and A. Mukherjee, Oxamusplatin: a cytotoxic Pt(ii) complex of a nitrogen mustard with resistance to thiol based sequestration displays enhanced selectivity towards cancer, *Dalton Trans.*, 2020, **49**(8), 2547–2558, DOI: 10.1039/C9DT04269E.

29 M. Manikandan, C. Sushanta, G. Shubhankar, P. Subhadee, V. Shreyas, K. Subhash, D. Prakash, K. Jyoti, I. Arvind, K. Ullas, P. Malay, *et al.*, Improving In Vivo Tumor Accumulation and Efficacy of Platinum Antitumor Agents by Electronic Tuning of the Kinetic Lability, *Chem. – Eur. J.*, 2023, e202302720, DOI: 10.1002/chem.202302720.

30 M.-C. Barth, S. Lange, N. Häfner, N. Ueberschaar, H. Görls, I. B. Runnebaum and W. Weigand, Synthesis and characterization of thiocarbonato-linked platinum(IV) complexes, *Dalton Trans.*, 2022, **51**(14), 5567–5576, DOI: 10.1039/D2DT00318J.

31 Y.-Z. Shu, J. Lin, B.-Q. Zhu, Q.-H. Liu, B. Zhou, H.-F. Hu and D.-W. Ju, Synthesis and Antitumor Activity of (3-Hydroxyacrylato-O,O′) Diammineplatinum(II), *Pharm. Fronts*, 2021, **03**(01), e13–e17, DOI: 10.1055/s-0041-1730956.

32 N. Summa, W. Schiessl, R. Puchta, N. van Eikema Hommes and R. van Eldik, Thermodynamic and Kinetic Studies on Reactions of Pt(II) Complexes with Biologically Relevant Nucleophiles, *Inorg. Chem.*, 2006, **45**(7), 2948–2959, DOI: 10.1021/ic051955r.

33 A. Hofmann, D. Jaganyi, O. Q. Munro, G. Liehr and R. van Eldik, Electronic Tuning of the Lability of Pt(II) Complexes

through π-Acceptor Effects. Correlations between Thermodynamic, Kinetic, and Theoretical Parameters, *Inorg. Chem.*, 2003, **42**(5), 1688–1700, DOI: 10.1021/ic020605r.

34 E. C. Sutton, C. E. McDevitt, J. Y. Prochnau, M. V. Yglesias, A. M. Mroz, M. C. Yang, R. M. Cunningham, C. H. Hendon and V. J. DeRose, Nucleolar Stress Induction by Oxaliplatin and Derivatives, *J. Am. Chem. Soc.*, 2019, **141**(46), 18411–18415, DOI: 10.1021/jacs.9b10319.

35 S. T. Chew, K. M. Lo, S. K. Sinniah, K. S. Sim and K. W. Tan, Synthesis, characterization and biological evaluation of cationic hydrazone copper complexes with diverse diimine co-ligands, *RSC Adv.*, 2014, **4**(106), 61232–61247, DOI: 10.1039/C4RA11716F.

36 D. L. Ang, C. Kelso, J. L. Beck, S. F. Ralph, D. G. Harman and J. R. Aldrich-Wright, A study of Pt(II)–phenanthroline complex interactions with double-stranded and G-quadruplex DNA by ESI-MS, circular dichroism, and computational docking, *JBIC, J. Biol. Inorg. Chem.*, 2020, **25**(3), 429–440, DOI: 10.1007/s00775-020-01773-4.

37 A. Annunziata, A. Amoresano, M. E. Cucciolito, R. Esposito, G. Ferraro, I. Iacobucci, P. Imbimbo, R. Lucignano, M. Melchiorre, M. Monti, *et al.*, Pt(II) versus Pt(IV) in Carbene Glycoconjugate Antitumor Agents: Minimal Structural Variations and Great Performance Changes, *Inorg. Chem.*, 2020, **59**(6), 4002–4014, DOI: 10.1021/acs.inorgchem.9b03683.

38 D. Jaganyi, A. Hofmann and R. van Eldik, Controlling the Lability of Square-Planar PtII Complexes through Electronic Communication between π-Acceptor Ligands, *Angew. Chem., Int. Ed.*, 2001, **40**(9), 1680–1683, DOI: 10.1002/1521-3773(20010504)40:9<1680::AID-ANIE16800>3.0.CO;2-K.

39 J. Bogojeski, ŽD. Bugarčić, R. Puchta and R. van Eldik, Kinetic Studies on the Reactions of Different Bifunctional Platinum(II) Complexes with Selected Nucleophiles, *Eur. J. Inorg. Chem.*, 2010, **2010**(34), 5439–5445, DOI: 10.1002/ejic.201000654.

40 J. Josephsen, Diaminehalogenoplatinum(II) complex reactions with DMSO, *Inorg. Chim. Acta*, 2018, **478**, 54–58, DOI: 10.1016/j.ica.2018.03.039.

41 A. M. Talarico, E. I. Szerb, T. F. Mastropietro, I. Aiello, A. Crispini and M. Ghedini, Tuning solid state luminescent properties in a hydrogen bonding-directed supramolecular assembly of bis-cyclometalated iridium(III) ethylenediamine complexes, *Dalton Trans.*, 2012, **41**(16), 4919–4926, DOI: 10.1039/C2DT12108E.

42 K. A. Mitchell and C. M. Jensen, Synthesis, Characterization, and Reactivity of Platinum Cysteinato and Related Thiolato Complexes: Molecular Structure of Pt2(.mu.-N-acetyl-L-cysteine-S)2(bpy)2, *Inorg. Chem.*, 1995, **34**(17), 4441–4446, DOI: 10.1021/ic00121a023.

43 T. Peega, R. N. Magwaza, L. Harmse and I. A. Kotzé, Synthesis and evaluation of the anticancer activity of [Pt(diimine)(N,N-dibutyl-N′-acylthiourea)]+ complexes, *Dalton Trans.*, 2021, **50**(34), 11742–11762, DOI: 10.1039/D1DT01385H.

44 V. Coccè, I. Rimoldi, G. Facchetti, E. Ciusani, G. Alessandri, L. Signorini, F. Sisto, A. Giannì, F. Paino and A. Pessina, In Vitro Activity of Monofunctional Pt-II Complex Based on 8-Aminoquinoline against Human Glioblastoma, *Pharmaceutics*, 2021, **13**(12), 2101.

45 D. Aiello, A. M. Talarico, F. Teocoli, E. I. Szerb, I. Aiello, F. Testa and M. Ghedini, Self-incorporation of a luminescent neutral iridium(III) complex in different mesoporous micelle-templated silicas, *New J. Chem.*, 2011, **35**(1), 141–148, DOI: 10.1039/C0NJ00533A.

46 M. La Deda, A. Grisolia, I. Aiello, A. Crispini, M. Ghedini, S. Belviso, M. Amati and F. Lelj, Investigations on the electronic effects of the peripheral 4′-group on 5-(4′-substituted)phenylazo-8-hydroxyquinoline ligands: zinc and aluminium complexes, *Dalton Trans.*, 2004, (16), 2424–2431, DOI: 10.1039/B404814H.

47 P. Skehan, R. Storeng, D. Scudiero, A. Monks, J. McMahon, D. Vistica, J. T. Warren, H. Bokesch, S. Kenney and M. R. Boyd, New Colorimetric Cytotoxicity Assay for Anticancer-Drug Screening, *J. Natl. Cancer Inst.*, 1990, **82**(13), 1107–1112, DOI: 10.1093/jnci/82.13.1107, (acccessed 5/3/2023).

48 M. J. Frisch, G. W. Trucks, H. B. Schlegel, G. E. Scuseria, M. A. Robb, J. R. Cheeseman, G. Scalmani, V. Barone, G. A. Petersson and H. Nakatsuji, *et al.*, *Gaussian 16 Rev. C.01*, 2016.

49 A. D. Becke, Density–functional thermochemistry. III. The role of exact exchange, *J. Chem. Phys.*, 1993, **98**(7), 5648–5652, DOI: 10.1063/1.464913, (acccessed 4/28/2023).

50 C. Lee, W. Yang and R. G. Parr, Development of the Colle-Salvetti correlation-energy formula into a functional of the electron density, *Phys. Rev. B: Condens. Matter Mater. Phys.*, 1988, **37**(2), 785–789, DOI: 10.1103/physrevb.37.785, From NLM.

51 S. Grimme, J. Antony, S. Ehrlich and H. Krieg, A consistent and accurate ab initio parametrization of density functional dispersion correction (DFT-D) for the 94 elements H-Pu, *J. Chem. Phys.*, 2010, **132**(15), 154104, DOI: 10.1063/1.3382344, From NLM.

52 D. Andrae, U. Häußermann, M. Dolg, H. Stoll and H. Preuß, Energy-adjustedab initio pseudopotentials for the second and third row transition elements, *Theor. Chim. Acta*, 1990, **77**(2), 123–141, DOI: 10.1007/BF01114537.

53 G. Scalmani and M. J. Frisch, Continuous surface charge polarizable continuum models of solvation. I. General formalism, *J. Chem. Phys.*, 2010, **132**, 114110, DOI: 10.1063/1.3359469.

54 H. Cartwright, Molecular Thermodynamics, By Donald A. McQuarrie and John D. Simon, (1999) University Science Books, 55D Gate Five Road, Sausalito CA 94965, USA. 672 pp $78.00, ISBN 1-891389-05-X, *Chem. Educ.*, 1999, **4**(3), 120–121, DOI: 10.1007/s00897990307a.

55 K. Fukui, The path of chemical reactions - the IRC approach, *Acc. Chem. Res.*, 1981, **14**(12), 363–368, DOI: 10.1021/ar00072a001.

56 H. P. Hratchian and H. B. Schlegel, *Theory and Applications of Computational Chemistry: The First 40 Years*, Elsevier, 2005.
57 R. Ditchfield, Self-consistent perturbation theory of diamagnetism, *Mol. Phys.*, 1974, **27**(4), 789–807, DOI: **10.1080/00268977400100711**.
58 F. London, Théorie quantique des courants interatomiques dans les combinaisons aromatiques, *J. Phys. Radium*, 1937, **8**(10), 397–409, DOI: **10.1051/jphysrad:01937008010039700**.
59 M. K. Cyrański, M. H. Jamróz, A. Rygula, J. C. Dobrowolski, Ł. Dobrzycki and M. Baranska, On two alizarin polymorphs, *CrystEngComm*, 2012, **14**(10), 3667–3676, DOI: **10.1039/C2CE06063A**.
60 T. F. Mastropietro, E. I. Szerb, M. La Deda, A. Crispini, M. Ghedini and I. Aiello, Cyclopalladated 3,5-Disubstituted 2-(2′-Pyridyl)pyrroles Complexed to 8-Hydroxyquinoline or 4-Hydroxyacridine, *Eur. J. Inorg. Chem.*, 2013, **2013**(12), 2188–2194, DOI: **10.1002/ejic.201201341**.
61 A. Ionescu, N. Godbert, R. Termine, M. La Deda, M. Amati, F. Lelj, A. Crispini, A. Golemme, M. Ghedini, P. Garcia-Orduña, *et al.*, Photoconductive Properties and Electronic Structure in 3,5-Disubstituted 2-(2′-Pyridyl)Pyrroles Coordinated to a Pd(II) Salicylideneiminate Synthon, *Inorg. Chem.*, 2021, **60**(13), 9287–9301, DOI: **10.1021/acs.inorgchem.0c02991**.
62 H.-Y. Jiang, X.-D. Hu, J.-J. Zhu, J. Wan and J.-B. Yao, Studies on the photofading of alizarin, the main component of madder, *Dyes Pigm.*, 2021, **185**, 108940, DOI: **10.1016/j.dyepig.2020.108940**.
63 J. H. de Araujo-Neto, A. P. M. Guedes, C. M. Leite, C. A. F. Moraes, A. L. Santos, R. d. S. Brito, T. L. Rocha, F. Mello-Andrade, J. Ellena and A. A. Batista, "Half-Sandwich" Ruthenium Complexes with Alizarin as Anticancer Agents: In Vitro and In Vivo Studies, *Inorg. Chem.*, 2023, **62**(18), 6955–6969, DOI: **10.1021/acs.inorgchem.3c00183**.
64 L. Zhu, Y.-L. Bai, Y. Zhao, F. Xing, M.-X. Li and S. Zhu, Bis(2-pyridylmethyl)amine-functionalized alizarin: an efficient and simple colorimetric sensor for fluoride and a fluorescence turn-on sensor for Al^{3+} in an organic solution, *Dalton Trans.*, 2019, **48**(15), 5035–5047, DOI: **10.1039/C9DT00859D**.
65 V. M. Miskowski and V. H. Houlding, Electronic spectra and photophysics of platinum(II) complexes with .alpha.-diimine ligands. Solid-state effects. 1. Monomers and ligand .pi. dimers, *Inorg. Chem.*, 1989, **28**(8), 1529–1533, DOI: **10.1021/ic00307a021**.
66 M. A. Ivanov, M. V. Puzyk and K. P. Balashev, Spectroscopic and electrochemical properties of dichlorodiimine complexes of Au(III) and Pt(II) with 1,4-diazine derivatives of o-phenanthroline, *Russ. J. Gen. Chem.*, 2006, **76**(6), 843–848, DOI: **10.1134/S1070363206060016**.
67 A. DelMedico, E. S. Dodsworth, A. B. P. Lever and W. J. Pietro, Electronic Structure and Spectra of Linkage Isomers of Bis(bipyridine)(1,2-dihydroxy-9,10-anthraquinonato)ruthenium(II) and Their Redox Series, *Inorg. Chem.*, 2004, **43**(8), 2654–2671, DOI: **10.1021/ic035370d**.
68 E. E. Langdon-Jones and S. J. A. Pope, The coordination chemistry of substituted anthraquinones: Developments and applications, *Coord. Chem. Rev.*, 2014, **269**, 32–53, DOI: **10.1016/j.ccr.2014.02.003**.
69 OECD Guideline for Testing of Chemicals-Partition Coefficient (n-octanol/water). High Performance Liquid Chromatography (HPLC) Method, 117, Adopted: 30.03.89.
70 J. J. Wilson and S. J. Lippard, In Vitro Anticancer Activity of cis-Diammineplatinum(II) Complexes with β-Diketonate Leaving Group Ligands, *J. Med. Chem.*, 2012, **55**(11), 5326–5336, DOI: **10.1021/jm3002857**.
71 J. A. Platts, S. P. Oldfield, M. M. Reif, A. Palmucci, E. Gabano and D. Osella, The RP-HPLC measurement and QSPR analysis of log $P_{o/w}$ values of several Pt(II) complexes, *J. Inorg. Biochem.*, 2006, **100**(7), 1199–1207, DOI: **10.1016/j.jinorgbio.2006.01.035**.
72 I. Tolbatov, D. Cirri, M. Tarchi, T. Marzo, C. Coletti, A. Marrone, L. Messori, N. Re and L. Massai, Reactions of Arsenoplatin-1 with Protein Targets: A Combined Experimental and Theoretical Study, *Inorg. Chem.*, 2022, **61**(7), 3240–3248, DOI: **10.1021/acs.inorgchem.1c03732**.
73 L. Massai, S. Ciambellotti, L. Cosottini, L. Messori, P. Turano and A. Pratesi, Direct detection of iron clusters in L ferritins through ESI-MS experiments, *Dalton Trans.*, 2021, **50**(45), 16464–16467, DOI: **10.1039/D1DT03106F**.
74 L. Massai, C. Zoppi, D. Cirri, A. Pratesi and L. Messori, Reactions of Medicinal Gold(III) Compounds With Proteins and Peptides Explored by Electrospray Ionization Mass Spectrometry and Complementary Biophysical Methods, *Front. Chem.*, 2020, **8**, 581648, DOI: **10.3389/fchem.2020.581648**.
75 I. Rombouts, B. Lagrain, K. A. Scherf, M. A. Lambrecht, P. Koehler and J. A. Delcour, Formation and reshuffling of disulfide bonds in bovine serum albumin demonstrated using tandem mass spectrometry with collision-induced and electron-transfer dissociation, *Sci. Rep.*, 2015, **5**(1), 12210, DOI: **10.1038/srep12210**.
76 G. Ferraro, L. Massai, L. Messori and A. Merlino, Cisplatin binding to human serum albumin: a structural study, *Chem. Commun.*, 2015, **51**(46), 9436–9439, DOI: **10.1039/C5CC01751C**.
77 F. Sacco, M. Tarchi, G. Ferraro, A. Merlino, G. Facchetti, I. Rimoldi, L. Messori and L. Massai, Reactions with Proteins of Three Novel Anticancer Platinum(II) Complexes Bearing N-Heterocyclic Ligands, *Int. J. Mol. Sci.*, 2021, **22**(19), 10551.
78 M. E. Alberto, V. Butera and N. Russo, Which One among the Pt-Containing Anticancer Drugs More Easily Forms Monoadducts with G and A DNA Bases? A Comparative Study among Oxaliplatin, Nedaplatin, and Carboplatin, *Inorg. Chem.*, 2011, **50**(15), 6965–6971, DOI: **10.1021/ic200148n**.
79 A. Ionescu, N. Godbert, L. Ricciardi, M. La Deda, I. Aiello, M. Ghedini, I. Rimoldi, E. Cesarotti,

G. Facchetti, G. Mazzeo, *et al.*, Luminescent water-soluble cycloplatinated complexes: Structural, photophysical, electrochemical and chiroptical properties, *Inorg. Chim. Acta*, 2017, **461**, 267–274, DOI: **10.1016/j.ica.2017.02.026**.

80 E. Dabbish, A. G. Ritacca, G. Mazzone and E. Sicilia, A comparative computational mechanistic study on derivatives of pyriplatin, modified with the –CH2Ph3P+ group, as anticancer complexes targeting mitochondria, *Inorg. Chim. Acta*, 2020, **512**, 119863, DOI: **10.1016/j.ica.2020.119863**.